Reductive metabolism increases the proinflammatory activity of aldehyde phospholipids[s]

Elena Vladykovskaya,[1] Evgeny Ozhegov,[1] J. David Hoetker, Zhengzhi Xie, Yonis Ahmed, Jill Suttles, Sanjay Srivastava, Aruni Bhatnagar, and Oleg A. Barski[2]

Diabetes and Obesity Center, School of Medicine, University of Louisville, Louisville, KY 40202

Abstract The generation of oxidized phospholipids in lipoproteins has been linked to vascular inflammation in atherosclerotic lesions. Products of phospholipid oxidation increase endothelial activation; however, their effects on macrophages are poorly understood, and it is unclear whether these effects are regulated by the biochemical pathways that metabolize oxidized phospholipids. We found that incubation of 1-palmitoyl-2-(5′-oxo-valeroyl)-sn-glycero-3-phosphocholine (POVPC) with THP-1-derived macrophages upregulated the expression of cytokine genes, including granulocyte/macrophage colony-stimulating factor (GM-CSF), tumor necrosis factor (TNF)-α, monocyte chemotactic protein 1 (MCP-1), interleukin (IL)-1β, IL-6, and IL-8. In these cells, reagent POVPC was either hydrolyzed to lyso-phosphatidylcholine (lyso-PC) or reduced to 1-palmitoyl-2-(5-hydroxy-valeroyl)-sn-glycero-3-phosphocholine (PHVPC). Treatment with the phospholipase A$_2$ (PLA$_2$) inhibitor, pefabloc, decreased POVPC hydrolysis and increased PHVPC accumulation. Pefabloc also increased the induction of cytokine genes in POVPC-treated cells. In contrast, PHVPC accumulation and cytokine production were decreased upon treatment with the aldose reductase (AR) inhibitor, tolrestat. In comparison with POVPC, lyso-PC led to 2- to 3-fold greater and PHVPC 10- to 100-fold greater induction of cytokine genes. POVPC-induced cytokine gene induction was prevented in bone-marrow derived macrophages from AR-null mice. These results indicate that although hydrolysis is the major pathway of metabolism, reduction further increases the proinflammatory responses to POVPC.[JLR] Thus, vascular inflammation in atherosclerotic lesions is likely to be regulated by metabolism of phospholipid aldehydes in macrophages.—Vladykovskaya, E., E. Ozhegov, J. D. Hoetker, Z. Xie, Y. Ahmed, J. Suttles, S. Srivastava, A. Bhatnagar and O. A. Barski. **Reductive metabolism increases the proinflammatory activity of aldehyde phospholipids.** *J. Lipid Res.* **2011.** 52: 2209–2225.

Supplementary key words macrophages • cytokines • POVPC • aldose reductase • phospholipase A$_2$ • gene expression

Cardiovascular diseases have become the leading cause of death in the world. A majority of cardiovascular diseases are due to atherosclerosis, which is underlying pathology associated with 70-75% of all cardiovascular deaths (1). Atherosclerosis is a chronic inflammatory state associated with the formation of characteristic vascular lesions rich in cholesterol, macrophages, and proliferating smooth muscle cells (2, 3). Occasionally, these plaques rupture or erode and thereby prevent blood flow to target tissue by forming occlusive thrombi. A key initiating event in the process of atherogenesis is the vascular recruitment of monocytes by lipoproteins trapped within the vessel wall. It is currently believed that once lodged within the subintimal space, the lipoproteins undergo nonenzymatic oxidation, which generates bioactive products that cause inflammation and promote monocyte recruitment. Investigations into the nature of these bioactive products have shown that most of the biological activity of oxidized lipoproteins could be attributed to the products of phospholipid oxidation generated within the lipoprotein particle (4, 5).

Oxidation of phospholipids results in the generation of several metastable end-products. In LDL, the most abundant products are those that are derived from the oxidation of 1-palmitoyl-2-arachidonoyl-sn-glycero-3-phosphocholine (PAPC). PAPC is the major phospholipid present in LDL, and the oxidation of its sn-2 arachidonic acid chain results in the formation of several carbonyl compounds of which 1-palmitoyl-2-(5′-oxo-valeroyl)-sn-glycero-3-phosphocholine (POVPC) (Scheme 1A) is generated in the highest

concentration (5). POVPC is the most reactive phospholipid generated in oxLDL, and the overall biological reactivity of oxLDL is dominated by its POVPC content (6).

Extensive evidence supports the view that POVPC and related phospholipids play an important role in atherogenesis. These phospholipids have been detected in oxidized LDL and atherosclerotic lesions of humans, rabbits, and mice (7, 8), and high titers of antibodies against POVPC and other lipid oxidation products develop in apoE-null mice (8). Significantly, the circulating levels of POVPC-bound apoB correlate strongly with coronary artery disease (9) and reflect the extent of carotid and femoral atherosclerosis (10), suggesting that the generation of oxidized phospholipids may be linked to disease progression. In vitro, POVPC activates endothelial cells to bind monocytes (5), and it increases the transcription of cytokine genes such as IL-8 and MCP-1 (11, 12); therefore, it could establish a chronic state of inflammation required for the initiation and the progression of atherosclerotic lesions (4, 13). Indeed, topical application of oxidized lipids to carotid arteries in mice increases vascular inflammation (14).

The high biological activity of POVPC and related phospholipids has been suggested to be due to the presence of a short chain at the *sn-2* position. This chain is recognized by several cellular receptors, and as a result, oxidized phospholipids can activate multiple signal transduction events. Our previous studies showed that the *sn-2* aldehydes are reduced by enzymes belonging to the aldo-keto reductase (AKR) superfamily (15). Of these enzymes, aldose reductase (AKR1B1, AR) was found to be particularly efficient in catalyzing the reduction of the *sn-2* aldehyde of POVPC to the corresponding alcohol. Nevertheless, it is not known whether metabolism via AR regulates the biological activity of phospholipid aldehydes. Accordingly, the current study was designed to develop a better under-

standing of the role of AR in regulating the proinflammatory effects of POVPC in macrophages. We chose to study macrophages because these cells have been shown to play an obligatory role in lesion development (16). Our results show that macrophages respond to POVPC by strongly upregulating the expression of several cytokine genes and that the induction of these genes is regulated by the metabolism of POVPC via AR.

MATERIALS AND METHODS

Reagents

1-palmitoyl-2-arachidonoyl-*sn*-glycero-3-phosphocholine was purchased from Avanti Polar Lipids (Alabaster, AL). Solvents and other analytical grade reagents were obtained from Sigma Chemical Co. (St. Louis, MO). POVPC, PHVPC, POVPE [1-palmitoyl-2-(5′-oxo-valeroyl)-*sn*-glycero-3-phosphoethanolamine], and PHVPE [1-palmitoyl-2-(5′-hydroxy-valeroyl)-*sn*-glycero-3-phosphoethanolamine] were synthesized as described previously (17). Purity of the phospholipid aldehydes was established by ESI^+/MS. Phospholipid concentration was determined by measuring inorganic phosphate or choline. Choline was measured using the Phospholipids C kit (Wako, Osaka, Japan), and inorganic phosphate was measured as described in (18). Pefabloc was purchased from Pentapharm (Basel, Switzerland). Tolrestat was a gift from American Home Products (Madison, NJ). Cell culture reagents were obtained from Invitrogen (Carlsbad, CA), and plates were from Corning (Union City, CA). RNeasy RNA isolation kit was from Qiagen (Valencia, CA), rDNase (DNA-free™ Kit) was from Ambion (Austin, TX), AMV Reverse Transcriptase from Promega (Madison, WI), and SYBR Green master mix from Quanta BioSciences (Gaithersburg, MD).
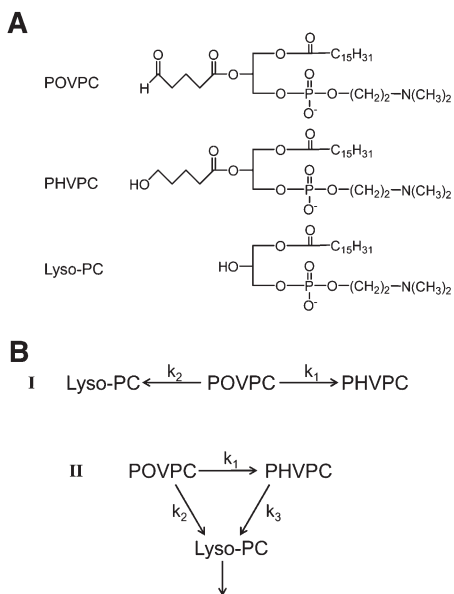
Cell culture

THP-1 cells obtained from the American Type Culture Collection (ATCC) were cultured in RPMI 1640 medium supplemented with 10% fetal bovine serum and 1% penicillin/streptomycin at 37°C and 5% CO_2 in a humidified incubator. For differentiation into the macrophage-like cells, phorbol 12-myristate 13-acetate (PMA) was added to a final concentration of 100 nM in growth media, and cells were incubated for 72 h. Immortalized murine macrophage cell lines were established by infecting the bone marrow of wild-type C57BL/6J mice and AR-null homozygous mice with the murine recombinant J2 retrovirus containing the v-myc and v-raf oncogenes as described (19). The resulting bone-marrow-derived macrophage cell lines were cultured in RPMI 1640 supplemented with 5% FBS, 1% HEPES, and 0.1% gentamycin.

To measure changes in the expression of cytokine genes, the cells (passages 4-10) were seeded in 6-well plates at 2 million cells per well in 2 ml of media. Before treatment, THP-1-derived macrophages (THP-1 DM) and BMDM were serum-starved overnight in media containing 0.1% FBS. Treatment reagents were dissolved in Hanks balanced salt solution (HBSS, pH 7.4, 20 mM HEPES, 135 mM NaCl, 5.4 mM KCl, 1.0 mM $MgCl_2$, 2.0 mM $CaCl_2$, 2.0 mM NaH_2PO_4, 5.5 mM glucose). For metabolic studies, the cells were seeded in 10 cm dishes at a density of 12 million per 10 ml media. For inhibitor experiments, the cells were preincubated in 2.5 ml media containing 50 μM inhibitor in HBSS for 1 h before POVPC addition. After incubation for indicated time, the cells were washed twice with HBSS, scraped, and resuspended in the lysis buffer.

Phospholipid analysis

Lipids were extracted from cells or media using the Bligh-Dyer procedure (20). Briefly, after washing twice with cold HBSS, the

A

POVPC

PHVPC

Lyso-PC

B

I   Lyso-PC $\xleftarrow{k_2}$ POVPC $\xrightarrow{k_1}$ PHVPC

II   POVPC $\xrightarrow{k_1}$ PHVPC
k_2 k_3
Lyso-PC

SCHEME 1. (A) Chemical structures of POVPC, PHVPC, and lyso-PC. (B) Potential pathways of chemical transformation of POVPC in macrophages.

cells were scraped from the plate in 0.9% NaCl in water and transferred into a glass tube; the volume was adjusted to 200 µl. To this, 500 µl methanol containing 750 pmol reagent 1,2-dicaproyl-*sn*-glycerophosphochline was added, followed by the addition of 250 µl chloroform. The solution was incubated at room temperature for 30 min with periodic mixing, after which another 250 µl chloroform and 250 µl 0.9% NaCl were added, and the phases were separated by brief centrifugation. The lower chloroform phase was analyzed by ESI/MS in positive and negative ionization modes using a Micromass ZMD 2000 mass spectrometer (Waters-Micromass, Milford, MA). 2:1 (v/v) methanol/chloroform containing 1% acetic acid was used as the flow injection solvent. Choline or phosphate content in each sample was measured, and phospholipids solutions were adjusted to equal concentration (2 µg inorganic phosphate per ml) prior to injection into the mass spectrometer. For the media extraction, 1.25 ml media was used, and all volumes were adjusted accordingly. Injections were carried out using a Harvard syringe pump at a flow rate of 20 µl per min. The ESI^+/MS operating parameters were as follows: capillary voltage, 3.38 kV; cone voltage, 25 V; extractor voltage, 9 V; RF lens voltage, 0.9 V; and source block and desolvation temperatures, 100 and 200°C, respectively. Nitrogen was used as the nebulizer gas at a flow rate of 3.4 l/h. Spectra were acquired at a rate of 275 atomic mass units per second over the mass range of 2-1,000 atomic mass units and were averaged over a period of 5 min or 100 scans. The amount of phospholipid was quantified using the ratio of the height of its peak to that of the standard (1,2-dicaproyl-*sn*-glycerophosphochline).

For the chemical identification of metabolites, LC-MS method was used. The phospholipid extract was injected into a Waters 1525 HPLC with a LiChrospher Si 60 (5 µm) 250-4 column preceded by a LiChrospher Si 60 (5 µm) guard column and eluted with an isocratic mobile phase consisting of 1 mM ammonium acetate in water:methanol:acetonitrile (15:8:77) at a flow rate of 1 ml/min followed by online monitoring by a Micromass ZMD 2000 mass spectrometer. The column eluent was split to collect the fractions (0.5 min each) simultaneously with MS detection. The fractions containing compounds of interest were analyzed with a Micromass Quattro LC mass spectrometer or with a Thermo Scientific LTQ-Orbitrap XL mass spectrometer.

In experiments with radioactive POVPC, POVPC labeled at the carbon-1 of the substituent at the *sn-2* position with ^{14}C was added to the incubation media (HBSS) at 1.2×10^{-7} Ci, 2.4 nmols per 2.5 ml. Lipids were separated from the media and the cells after incubation using the same procedure. Radioactivity was measured in both chloroform and aqueous phases using a Beckman liquid scintillation counter.

For synthesizing ^{14}C-POVPC, 4-bromo-1-1-dimethoxy butane (0.45 mmol) was stirred with 0.5 mmol ^{14}C-KCN (25 mCi, 50 mCi/mmol) in dimethyl formamide for 48 h. The resultant ^{14}C-5,5-dimethoxy pentanitrile was purified by column chromatography (Silica Gel 60, 35-75 µm, 15% ethyl acetate, 85% hexane) and hydrolyzed to yield ^{14}C-5,5-dimethoxy pentanoic acid under alkaline conditions (KOH, pH 12). Structure of ^{14}C-5,5-dimethoxy pentanoic acid was confirmed by NMR spectroscopy. The ^{14}C-5,5-dimethoxypentanoic acid was coupled with lyso-phosphatidylcholine (lyso-PC) to obtain ^{14}C-POVPC acetal as described previously (15, 17). Prior to use the ^{14}C-POVPC acetal was hydrolyzed by amberlite-15 (in acetone:water; 6:1 v/v) to yield ^{14}C-POVPC.

qRT-PCR

RNA was isolated using QIAGEN RNeasy kit, according to manufacturer's instructions, and treated with rDNase. RNA concentration was measured using the Nanodrop® 1000A Spectrometer. cDNA was synthesized from 1 µg RNA at 42°C for 1 h using oligo(dT)$_{12-18}$ primers and AMV Reverse Transcriptase. qRT PCR were performed in iCycler equipment (Bio-Rad) using SYBR Green detection. The following program was used in cDNA amplifications: 50°C for 2 min, 95°C for 10 min, 40 cycles of 95°C (denature) for 3 s, with 60°C for 20 s (annealing and extension). In parallel, GAPDH was amplified as endogenous control and reference gene. Amplification efficiency was verified for each pair of primers using a standard curve constructed by serial 10× dilution of control template. Relative fold increase in gene expression was calculated as $2^{-\Delta\Delta C(t)}$, where $\Delta\Delta C_t = \Delta C_{t,sample} - \Delta C_{t,control}$ and ΔC_t = (number of cycles needed to achieve threshold level for gene of interest) − (number of cycles needed to achieve threshold level for GAPDH). Human IL-6, granulocyte/macrophage colony-stimulating factor (GM-CSF), and mouse HPRT1 primers were from SABiosciences (Frederick, MD). Other primers were designed in-house or taken from published literature and are listed in supplementary Table I.

PCR array

Differentiated THP-1 cells were serum-starved as described above and treated in HBSS with or without POVPC for 3 h. cDNA was synthesized from 1 µg pooled RNA from six control and six treated samples obtained in two independent experiments. Human Signal Transduction PathwayFinder PCR Array and SYBR Green real-time PCR master mixes were from SABiosciences. Genomic DNA contamination assay incorporated on PCR assay plate did not detect genomic DNA contamination in control and test samples. Purity of used RNA and the efficiency of RT-PCR were confirmed by Positive PCR Control Test set on array. RT-PCR was performed using iCycler iQTM (Bio-Rad) with the following program: enzyme activation step of 95°C for 10 min was followed by 40 PCR cycles of denaturation at 95°C for 15 s and anneal/extension at 60°C for 1 min. For validating the PCR products, dissociation curve analysis was done immediately after RT-PCR. To accurately reflect the quantity of PCR products, baselines and threshold values were manually adjusted, and threshold values were set the same for control and test PCR arrays. A gene was eliminated from analysis when C_t exceeded 35 cycles. Data were analyzed using PCR Array Data Analysis web portal. Five housekeeping genes, B2M, HPRT1, RPL13A, GAPDH, and ACTB, were used for normalizing data.

Statistical analysis

Data are expressed as mean ± SEM. Comparisons were performed using one-way ANOVA for multiple comparisons or Student *t*-test for unpaired data. Statistical significance was accepted at $P < 0.05$.

RESULTS

POVPC induces expression of proinflammatory cytokines

Previous studies show that treatment of endothelial cells with POVPC results in the activation of proinflammatory signaling (13). However, the effects of POVPC on macrophages are poorly understood. Although it has been reported that free apoB-bound POVPC is a ligand of the scavenger receptor (CD36) (21), it is unclear how POVPC affects the expression of cytokine genes in macrophages. Hence, we studied the effects of POVPC on the expression of genes involved in macrophage signaling and cytokine production. For this, THP-1-derived macrophages were treated with 10 µM POVPC, and 3 h after treatment, gene expression was measured using a RT^2*Profiler*^{TM} PCR array.

As shown in **Fig. 1**, treatment with POVPC tended to induce rather than suppress gene expression. Detectable PCR products were obtained for 75 of 89 genes in POVPC-treated THP-1 cells (defined as requiring <35 cycles) and in 72 of 89 genes in untreated cells. The expression of the 5 housekeeping genes (B2M, HPRT1, RPL13A, GAPDH, and ACTB) was not affected. Altogether, treatment with POVPC led to the upregulation of 20 genes, whose expression was increased >2.5-fold; the expression of 4 genes was repressed by >2.5-fold (**Table 1** and supplementary Table II). As listed in Table 1, the expression of several inflammatory genes was increased from 10- to 100-fold. The most inducible genes were proinflammatory cytokines such as GM-CSF, TNF-α, and IL-8, and the expression of these genes was increased 100-, 60-, and 50-fold, respectively. Significant increases were also observed in the expression of cyclooxygenase 2 (COX-2), vascular cell adhesion molecule (VCAM)-1, matrix metallopeptidase (MMP)-1, TRAF2, and IL-1α. Collectively, these data indicate that POVPC establishes a proinflammatory state in macrophages characterized by the induction of genes regulated by the nuclear factor kappa (NF-κ)B pathway, leading to the upregulation of cytokines, chemokines, and COX-2. Given that TNF-α and IL-8 were most responsive to POVPC, we examined changes in these genes to study how metabolism regulates inflammation.

Metabolites of POVPC generated in THP-1 macrophages

To assess how POVPC-induced changes in proinflammatory genes are regulated by metabolism, we investigated POVPC metabolism in macrophages. For this, we identified the major POVPC metabolites generated in macrophages and the metabolic pathways involved in their
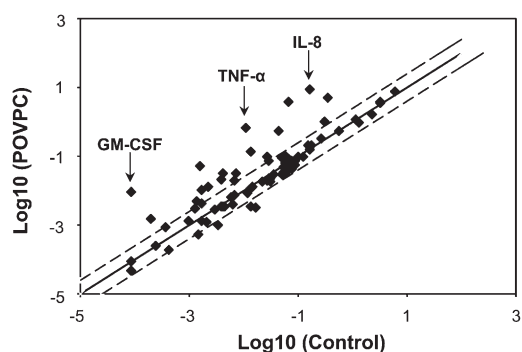

Fig. 1. POVPC-induced changes in gene expression in THP-1DM. Differentiated THP-1DM were serum-starved for 24 h and treated with or without 10 µM POVPC for 3 h in HBSS. Total RNA was isolated and cleaned with rDNase. RNA from 6 untreated and 6 POVPC-treated THP-1DM was pooled and reverse transcribed into cDNA. The RT^2 Profiler PCR Array was used to quantify changes in gene expression as described in *Materials and Methods*. The graph shows abundance and expression level of 89 genes in POVPC-treated cells versus untreated (control) cells. Data are expressed as arbitrary units on a log scale. Axes show relative abundance of the transcripts in control (abscissa) and treated (ordinate) samples. Dashed lines represent the 2.5 boundary values for fold induction.

generation. We also studied the interrelationship between these pathways.

To identify metabolites, serum-starved differentiated THP-1 cells were incubated with 10 µM POVPC. After the indicated duration of incubation, the cells were lysed, and their phospholipids were extracted by the Bligh and Dyer procedure and analyzed by ESI$^+$/MS. In naïve, untreated cells, several phospholipid ions were identified, but only background intensity at m/z 594 was observed, indicating that there is little or no POVPC in these cells under basal conditions (**Fig. 2A**). Treatment with POVPC for 15 min, however, led to the appearance of an ion with m/z 594 (Fig. 2A), indicating rapid cellular uptake of POVPC. Following 5 min of incubation with 2 nmol POVPC/10^6 cells, the cell content of POVPC constituted half of that of the media, with only 12% of added POVPC (25 nmol) detectable in the cells and the media combined, indicating that the compound is rapidly metabolized. Longer incubation periods led to a further decrease in POVPC levels and higher percentage found in the cells, consistent with the notion that POVPC is extracted from the media into the cells, where metabolic transformations take place.

The uptake of POVPC was accompanied by the emergence of another ion with m/z 596, indicating that in THP-1-derived macrophages, POVPC is metabolically reduced into 1-palmitoyl-2-hydroxyvaleroyl-phosphatidylcholine (PHVPC). In addition to metabolic transformation to PHVPC, POVPC could also be converted to lyso-PC either nonenzymatically or by phospholipase A$_2$ (PLA$_2$)-catalyzed hydrolysis. POVPC could also be oxidized to 1-palmitoyl-2-glutatoryl-3-phosphatidylcholine (PGPC). However, PGPC (m/z 610) was not formed in these cells, indicating that oxidation is not a metabolic fate of POVPC in these cells. Lyso-PC (m/z 496) was present in these cells even in the absence of POVPC treatment, and addition of POVPC led to a transient increase in the intensity of the 496 ion (Fig. 2A).

To establish chemical identity of POVPC metabolites, the phospholipid extract from the cells was separated by HPLC and the ions at m/z 496, 594, and 596 were followed using the online mass spectrometer. The retention times and the separation pattern matched closely with those of the standard compounds (Fig. 2B). The fractions corresponding to the peaks were collected and applied for MS/MS analysis in the positive and negative modes. The fragmentation patterns were identical to those of reagent standards (Fig. 2C). Specifically, in the negative mode, the fragments of the precursor ions ([M-15]$^-$, corresponding to the loss of a methyl group) were found at m/z 255 (*sn*-1 palmitate), m/z 115 (*sn*-2 substituent of POVPC: oxovaleroate) or m/z 117 (*sn*-2 of PHVPC: hydroxyvaleroate), and m/z 480 (lyso-PC) (Fig. 2C). In agreement with the literature (22), the *sn*-2 acyl fragment displayed higher intensity than that of *sn*-1. In the positive mode performed with a high-resolution mass spectrometer, the molecular ions [M+H]$^+$ of the analytes correspond to their theoretical mass-to-charge ratios (deviations less than 2.5 ppm), confirming the elemental composition of the compounds. All three compounds yielded a fragment with m/z 184.073, which is characteristic for phosphatidylcholines and

TABLE 1.   RT-PCR array results showing >2.5-fold up- and downregulation of cell signaling genes by POVPC

RefSeq	Symbol	Description	Gene Name	Fold Change (POVPC/Control)
Upregulated genes				
NM_000758	CSF2	Colony stimulating factor 2 (granulocyte-macrophage)	GMCSF	108.38
NM_000594	TNF	Tumor necrosis factor (TNF superfamily, member 2)	DIF/TNF-α	62.25
NM_004591	CCL20	Chemokine (C-C motif) ligand 20	CKb4/LARC	58.08
NM_000584	IL8	Interleukin 8	3-10C/AMCF-I	54.19
NM_001165	BIRC3	Baculoviral IAP repeat-containing 3	AIP1/API2	33.36
NM_000201	ICAM1	Intercellular adhesion molecule 1 (CD54), human rhinovirus receptor	BB2/CD54	14.52
NM_003398	NFKB1	Nuclear factor of kappa light polypeptide gene enhancer in B-cells 1 (p105))	DKFZp686C01211/EBP-1	12.64
NM_004049	BCL2A1	BCL2-related protein A1	ACC-1/ACC-2	10.27
NM_000963	PTGS2	Prostaglandin-endoperoxide synthase 2 (prostaglandin G/H synthase and cyclooxygenase)	COX-2/COX2	7.78
NM_001078	VCAM1	Vascular cell adhesion molecule 1	CD106/DKFZp779G2333	7.78
NM_002425	MMP10	Matrix metallopeptidase 10 (stromelysin 2)	SL-2/STMY2	6.32
NM_002467	MYC	V-myc myelocytomatosis viral oncogene homolog (avian)	c-Myc	5.90
NM_002982	CCL2	Chemokine (C-C motif) ligand 2	GDCF-2/GDCF-2 HC11	5.50
NM_001200	BMP2	Bone morphogenetic protein 2	BMP2A	4.47
NM_020182	TMEPAI	Transmembrane, prostate androgen induced RNA	PMEPA1/STAG1	3.63
NM_003376	VEGFA	Vascular endothelial growth factor A	VEGF/VEGF-A	3.63
NM_000598	IGFBP3	Insulin-like growth factor binding protein 3	BP-53/IBP3	3.39
NM_001166	BIRC2	Baculoviral IAP repeat-containing 2	API1/HIAP2	2.95
NM_004180	TANK	TRAF family member-associated NFKB activator	I-TRAF/TRAF2	2.57
NM_000575	IL1A	Interleukin 1, α	IL-1A/IL1	2.57
Downregulated genes				
NM_005522	HOXA1	Homeobox A1	BSAS/HOX1	0.37
NM_003006	SELPLG	Selectin P ligand	CD162/CLA	0.30
NM_000264	PTCH1	Patched homolog 1 (Drosophila)	BCNS/HPE7	0.26
NM_130851	BMP4	Bone morphogenetic protein 4	BMP2B/BMP2B1	0.20

corresponds to the phosphocholine moiety (not shown). Taken together, matching retention times on the HPLC and fragmentation patterns confirm unequivocal assignment of the chemical identity of the POVPC metabolites in THP-1 macrophages to PHVPC and lyso-PC.

Although addition of POVPC led to a transient increase in the intensity of the ion with an m/z value of 496, this change could not be rigorously attributed to POVPC metabolism, as this ion was present in the untreated cells. Hence, to identify the role of hydrolysis, we synthesized ^{14}C-POVPC to assay cellular PLA$_2$ activity. In this phospholipid, carbon 1 of the sn-2 chain was radiolabeled. Hence, hydrolysis by PLA$_2$ would be expected to result in the loss of the label from the cell and the appearance of hydrophilic, radioactive glutaryl-semialdehyde into the medium.

To assay hydrolysis, the cells were incubated with ^{14}C-POVPC (1.2×10^{-7} Ci, 2.4 nmol in 25 nmol total POVPC per 2.5 ml), and after 5 or 30 min of incubation, the cells and the medium were collected separately. Each of these was then extracted using the Bligh and Dyer procedure, and radioactivity in both the aqueous and the chloroform extracts of each fraction was measured. Our results showed that after 5 min of incubation, 61% of total radioactivity (cells + media) was in the aqueous extract and the rest in the chloroform fraction, indicating that POVPC was incorporated in the cells and readily hydrolyzed. The excised sn-2 chain was then extruded from the cells into the medium (**Fig. 3A**). After 30 min of incubation, 83% of the radioactivity was associated with aqueous extract of the medium (Fig. 3A). In the chloroform fraction, the ratio of radioactivity found in the medium to that in cells was 2:1,

indicating that most of the POVPC was sequestered in cells (the volume of cells is several orders of magnitude smaller than the volume of the media), whereas cleaved product, glutaryl semialdehyde, is present mostly in media. Mass spectrometric measurements of phospholipids in the cell and media extracts after 5 and 30 min of treatment showed distribution of POVPC between the cells and the media matching radioactivity measurements in the chloroform fraction (Fig. 3B). Between 5 and 30 min, there was a significant decrease in the amount of cell-associated radioactivity; consistent with the view that ^{14}C-glutaryl semialdehyde generated by hydrolysis is extruded from the cells to the medium. Collectively, these results indicate that in THP-1 macrophages, reduction and hydrolysis are the two major pathways of POVPC metabolism and that ultimately most (>80%) of POVPC is hydrolyzed to lyso-PC.

Biochemical pathways of POVPC metabolism

Conversion of POVPC to PHVPC and lyso-PC may be due to two independent competing pathways (Scheme 1B-I) or to a series of interdependent metabolic transformations (Scheme 1B-II), in which conversion to PHVPC may ($k_2 = 0$) or may not ($k_2 \neq 0$) be required for hydrolysis. To distinguish between these possibilities, the cells were pretreated with pefabloc, an inhibitor of PLA$_2$, to examine whether PLA$_2$ inhibition would affect POVPC reduction. The rate of hydrolysis was determined from the difference in radioactive counts in the chloroform fraction remaining after 5 and 30 min incubation (Fig. 3C). As expected, inhibition of PLA$_2$ reduced the rate of POVPC hydrolysis. In addition, as shown in **Fig. 4A**, pefabloc increased the intracellular accumulation of both POVPC and PHVPC, leading to an
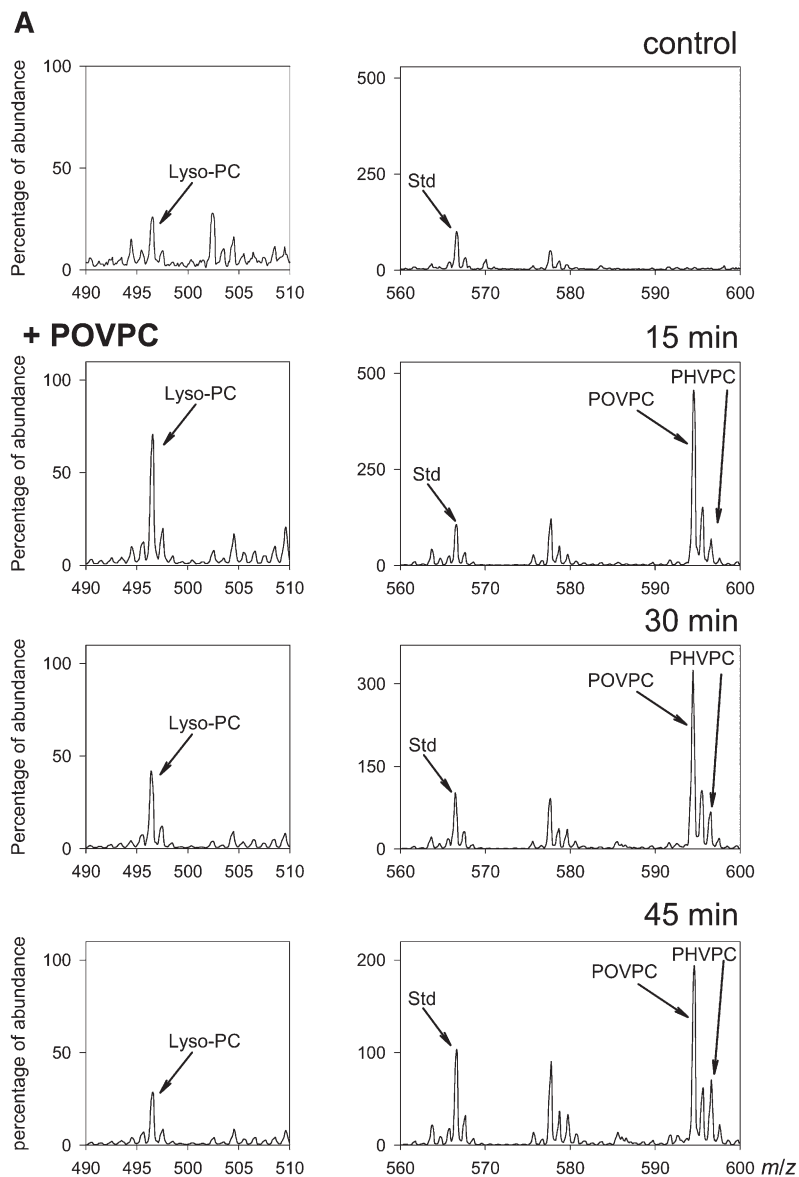
Fig. 2. Metabolism of POVPC in THP-DM. (A) ESI$^+$/MS mass spectra of the chloroform:methanol extract of THP-1 cells that were either left untreated (control) or treated with 10 μM POVPC for 15, 30, or 45 min. For each measurement, the cells were seeded in 10 cm dishes and treated as described in *Materials and Methods*. After 24 h of serum starvation, the medium was changed to HBSS containing 5.5 mM glucose. After 1 h of incubation in the buffer, the cells were treated with 10 μM POVPC in 5 ml HBSS for indicated times. At the end of incubation, the cells were lyzed, 1,2-dicaproyl-*sn*-glycerophosphochline was added as standard, and the phospholipids were extracted using the Bligh and Dyer procedure. Phospholipids solutions were adjusted to equal concentration (2 μg inorganic phosphate per ml). The ion abundance in all panels was normalized by the standard (100%) to allow comparison. Ions corresponding to POVPC and its metabolites PHVPC and lyso-PC are indicated; (B) LC-MS profile of reagent lyso-PC (i), POVPC (ii), and PHVPC (iii), and a phospholipid extract of THP-1 macrophages (iv–vi) treated with 50 nmol POVPC for 45 min. The asterisk * indicates an isotopic peak of POVPC. (C) HPLC fractions at indicated retention times (RT) were collected and analyzed by MS/MS in the negative ionization mode. Left column shows MS/MS spectra of the main [M-CH$_3$]$^-$ ion species at *m/z* 480.4 (i), 578.4 (ii) and 580.3 (iii) of reagent lyso-PC, POVPC, and PHVPC, respectively. The insets show the assignment of the product ions. The ion at *m/z* 255.1 is assigned to palmitate anion at the *sn-1* position of all three compounds; ions at *m/z* 115.0 (ii) and 117.0 (iii) are assigned to the oxovaleroate and hydroxyvaleroate anions at the *sn-2* position of POVPC and PHVPC, respectively; ion at *m/z* 480.3 arises from *sn-2* lyso-PC anion. Right panels show fragmentation pattern of fractions corresponding to HPLC peaks with *m/z* 496 (iv), *m/z* 594 (v), and *m/z* 596 (vi) collected from the sample extracted from POVPC-treated cells at indicated retention times.

increase in the PHVPC:POVPC ratio by 25% within 15 min (Fig. 4B, C). After 30 min, the levels of PHVPC in the cells exceeded those of POVPC (Fig. 4D), indicating that inhibition of hydrolysis decreases the metabolism of both POVPC and PHVPC. These observations are consistent with a scheme in which reduction and hydrolysis are competing pathways of POVPC metabolism, and therefore, inhibition of one pathway (hydrolysis) increases metabolism by the other pathway (reduction).

Next, we examined the reductive metabolism of POVPC. Our previous studies show that several AKRs can catalyze POVPC reduction (15). Although these enzymes show wide tissue distribution, AKR1B1 (AR) is the major AKR expressed in THP-1 cells (data not shown). To study the role of this enzyme, the cells were treated with the AR inhibitor tolrestat. Treatment with tolrestat inhibited the reduction of POVPC to PHVPC in these cells, reflected by a significant decrease in the PHVPC:POVPC ratio (Fig. 4A–C). Tolrestat, however, had only a minor (but positive) effect on hydrolysis (Fig. 3C), suggesting that both POVPC

and PHVPC undergo hydrolysis with a similar efficiency and the hydrolysis of POVPC may occur somewhat faster than hydrolysis of PHVPC. Taken together, these data suggest that PLA$_2$ and AR are the major enzymes involved in the metabolism of POVPC in THP-1 macrophages and that both hydrolysis and reduction compete with each other so that inhibition of hydrolysis increases POVPC reduction.

The observation that pefabloc increased the levels of unmetabolized POVPC indicates that PLA$_2$-induced hydrolysis is a significant route of POVPC metabolism. Treatment with tolrestat, however, did not lead to a statistically significant increase in unmetabolized POVPC. This suggests that k$_2$ is greater than k$_1$, but it does not help in distinguishing between Scheme 1B-I and Scheme 1B-II or in assessing whether PHVPC is also metabolized by PLA$_2$ (k$_3$ ≠ 0). Hence, to examine how PHVPC is metabolized, we synthesized reagent PHVPC. Treatment of THP-1 cells with PHVPC led to a rapid incorporation of reagent in membrane phospholipids (**Fig. 5A**). A gradual decrease in

B

Reagents

(i) *SIR m/z 496* — Lyso-PC

(ii) *SIR m/z 594* — POVPC

(iii) *SIR m/z 596* — PHVPC

Cell extract

(iv) *SIR m/z 496*

(v) *SIR m/z 594*

(vi) *SIR m/z 596*

C

(i) Lyso-PC — 255.2, 480.4

(ii) POVPC — 115.0, 255.1, 480.2, 578.4

(iii) PHVPC — 117.0, 255.1, 480.2, 580.3

(iv) RT: 31.8 min — 255.1, 480.4

(v) RT: 25.0 min — 115.0, 255.1, 480.2, 578.4

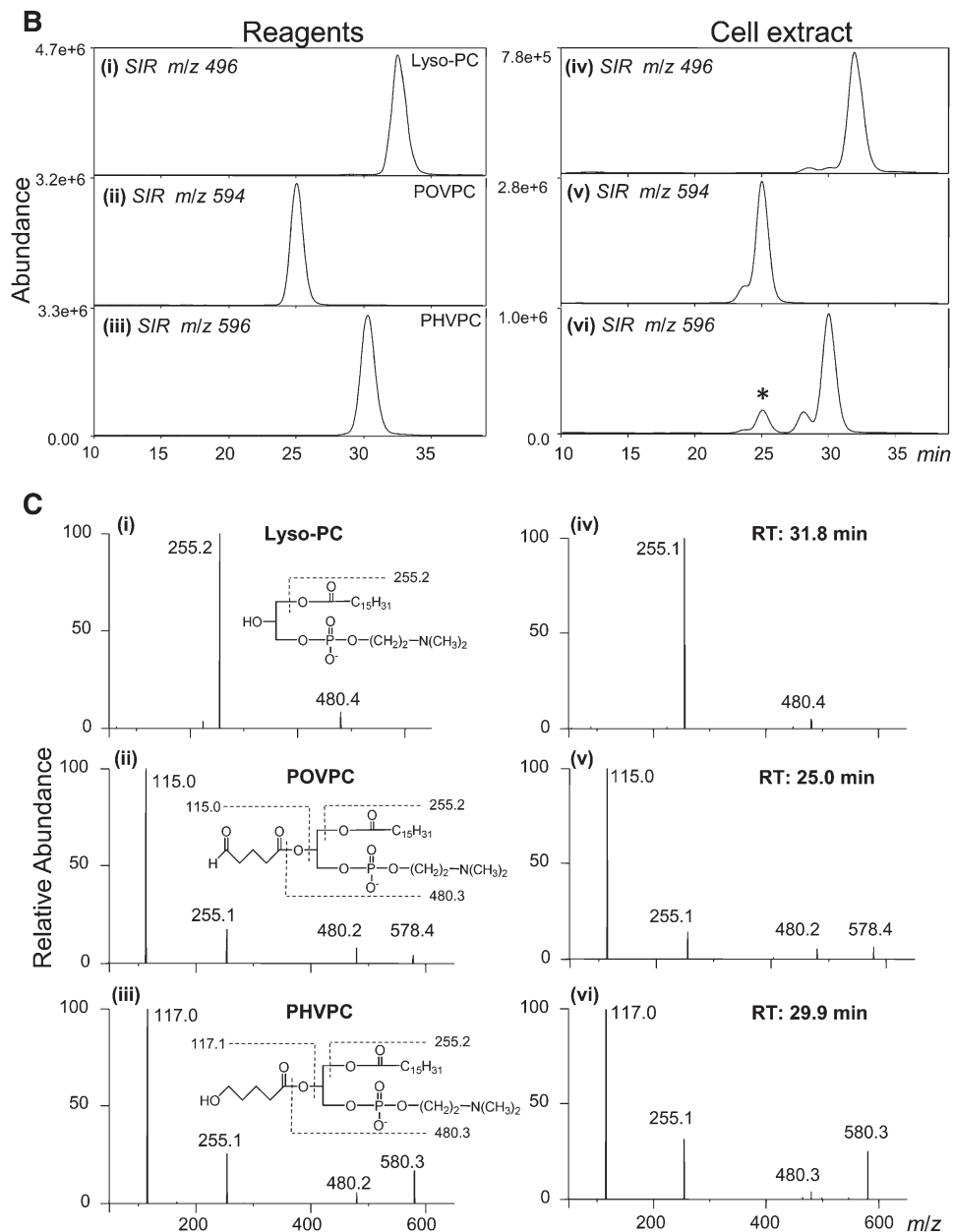(vi) RT: 29.9 min — 117.0, 255.1, 480.3, 580.3

Fig. 2.—*Continued.*

PHVPC content in the cells indicated that it is either metabolized or extruded. To identify whether it is metabolized, the cells were treated with pefabloc before incubation with PHVPC. As shown in Fig. 5A (right panel), treatment with pefabloc led to gradual build-up of unmetabolized PHVPC in the membrane, indicating that like POVPC, PHVPC is also metabolized by PLA_2. This conclusion supports the view that POVPC metabolism follows Scheme 1B-II. Moreover, a comparison of the rate of disappearance of POVPC and PHVPC in THP-1 showed that after exogenous addition, the rate of disappearance of POVPC was faster than that of PHVPC, indicating that POVPC is more rapidly metabolized than PHVPC (i.e., $k_2 > k_3$) (Fig. 5B).

Proinflammatory effects of POVPC and its metabolites: Extensive conversion of POVPC into lyso-PC and PHVPC suggests that the structural transformations induced by this metabolism might significantly affect the biological activity of the parent phospholipid. AR-catalyzed reduction could decrease the chemical reactivity of the *sn*-2 carbonyl, whereas PLA_2-mediated hydrolysis, which generates a lyso-phospholipid, could impart new activity to the molecule. Hence, to determine how metabolic conversion affects the biological activity of POVPC, we examined the relative efficacy of POVPC, PHVPC, and lyso-PC in inducing the expression of the cytokine genes. For this, we selected the genes (TNF-α, IL-8, GM-CSF, IL-1β, MCP-1, and IL-6) that were most strongly induced by POVPC (Table 1). Because we expected temporal variation in the extent of induction, we measured time-dependent changes in gene expression. As shown in **Fig. 6**, treatment with POVPC led to a rapid increase in the mRNA for TNF-α, IL-8, GM-CSF, and IL-1β. The earliest increase was observed with TNF-α. Maximal induction of the TNF-α gene was observed within
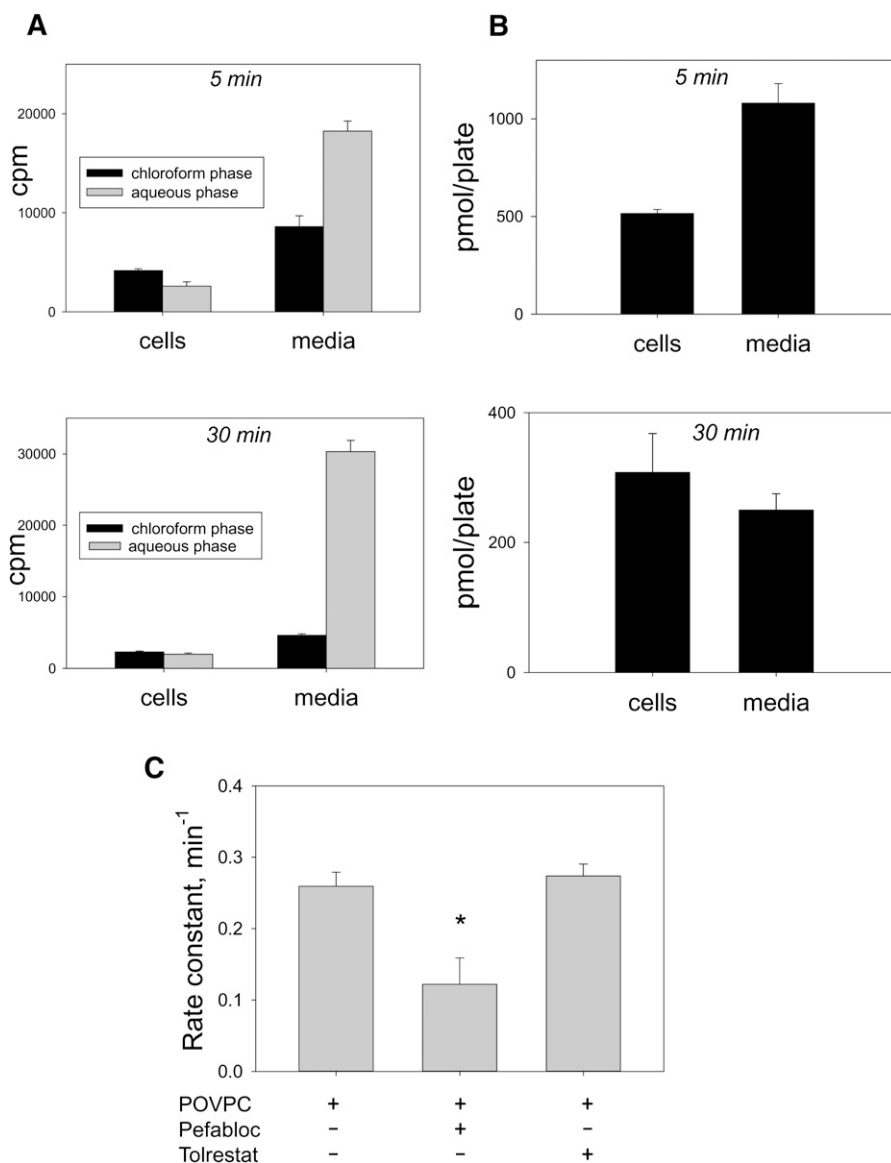
Metabolism of oxidized phospholipids   2215

Fig. 3. *sn*-2 hydrolysis of POVPC in THP-DM. (A) Serum-starved THP-DM were incubated in HBSS with C-1,^{14}C- POVPC for 5 or 30 min. After incubation, phospholipids were extracted using the Bligh and Dyer procedure from both the cells and the medium. Radioactivity was measured in both the chloroform and the aqueous fractions. (B) Amount of POVPC+PHVPC in the cells and the media were determined by mass spectrometry as described in *Materials and Methods*. (C) Effect of inhibitors on the rate of POVPC hydrolysis. The pseudo first-order rate constant was calculated as the difference between the logarithmic values of radioactivity counts in the chloroform fraction after 5 and 30 min incubation, divided by the time interval (25 min).

45-90 min of treatment with POVPC. The induction of TNF-α was followed by IL-8, GM-CSF, and IL-1β. The increase in the expression of all of these genes displayed nearly maximal induction within 90 min, indicating that these were the early-response genes. The expressions of the genes for MCP-1 and IL-6 were increased more slowly, potentially as part of a delayed early response.

In comparison with POVPC, PHVPC and lyso-PC were more effective in increasing the expression of cytokine genes. For example, in cells incubated with POVPC for 45 min, there was a 4- to 7-fold increase in IL-8 and TNF-α; however, in the presence of lyso-PC, the expression of these genes was increased 18- to 33-fold versus untreated cells (Fig. 6A, B). PHVPC was even more effective. In cells treated with PHVPC, 33- to 147-fold increase in the expression of both IL-8 and TNF-α was observed. Similar effects were observed with other cytokine genes. In untreated cells, the expression of GM-CSF (CSF2) was near the limits of detection. Treatment with POVPC for 3 h led to 38-fold increase in the expression of this gene. Under the same conditions, PHVPC was 36 times more potent in inducing GM-CSF than POVPC. Lyso-PC displayed intermediate reactivity (Fig. 6C). Similarly, the expression of IL-1β was increased 2- to 5-fold in cells treated with POVPC or lyso-PC, whereas treatment with PHVPC led to 30-fold increase in the expression of this gene with 90 min of treatment.
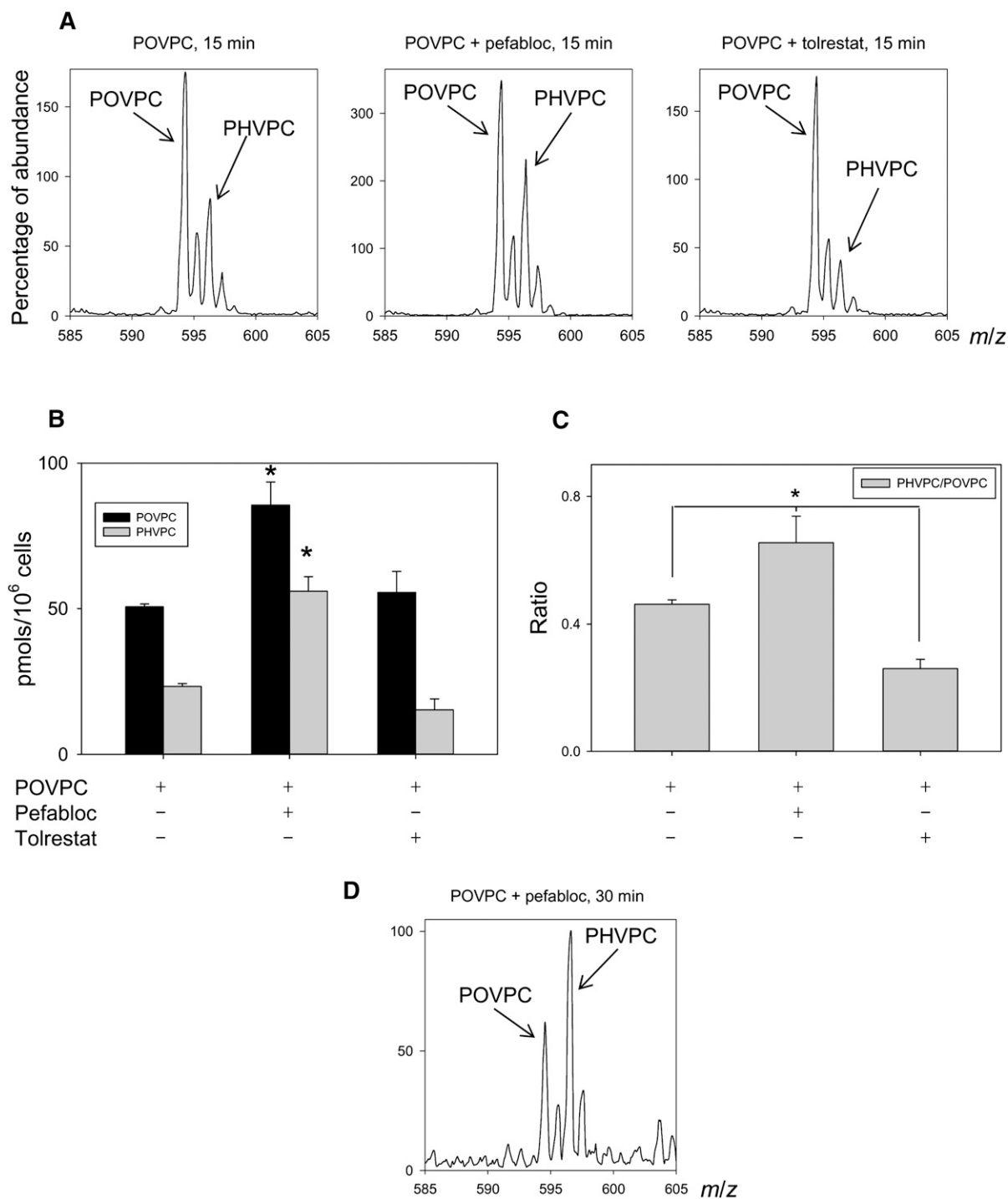
Fig. 4. Biochemical pathways for POVPC metabolism in THP-DM. (A) Effect of pefabloc and tolrestat on the ESI$^+$/MS mass spectra of the chloroform:methanol extract of THP-1 cells treated with 10 μM POVPC in 2.5 ml HBSS for 15 min. After 24 h of serum starvation, the cells were preincubated for 1 h in 50 μM pefabloc or 50 μM tolrestat before the addition of POVPC. After indicated durations of incubation, the cells were lyzed, and their phospholipids were extracted using the Bligh and Dyer procedure. Mass spectra were obtained as described in Fig. 2 legend and normalized to the intensity of the peak of the standard. Arrows indicate molecular ions due to unmetabolized POVPC and its metabolic product PHVPC. (B) Abundance of POVPC and PHVPC in THP-DM following 15 min treatments with 10 μM POVPC in 2.5 ml HBSS with or without 50 μM pefabloc or 50 μM tolrestat. The concentrations of POVPC and PHVPC were determined using 1,2-dicaproyl-*sn*-glycerophosphocholine as the standard. (C) Ratio of PHVPC to POVPC calculated from panel B. Data are mean ± SEM. (n = 3); *$P < 0.01$ versus cells treated with POVPC alone. (D) Mass spectrum of cell lipid extract treated with POVPC as in (A) in the presence of pefabloc for 30 min.
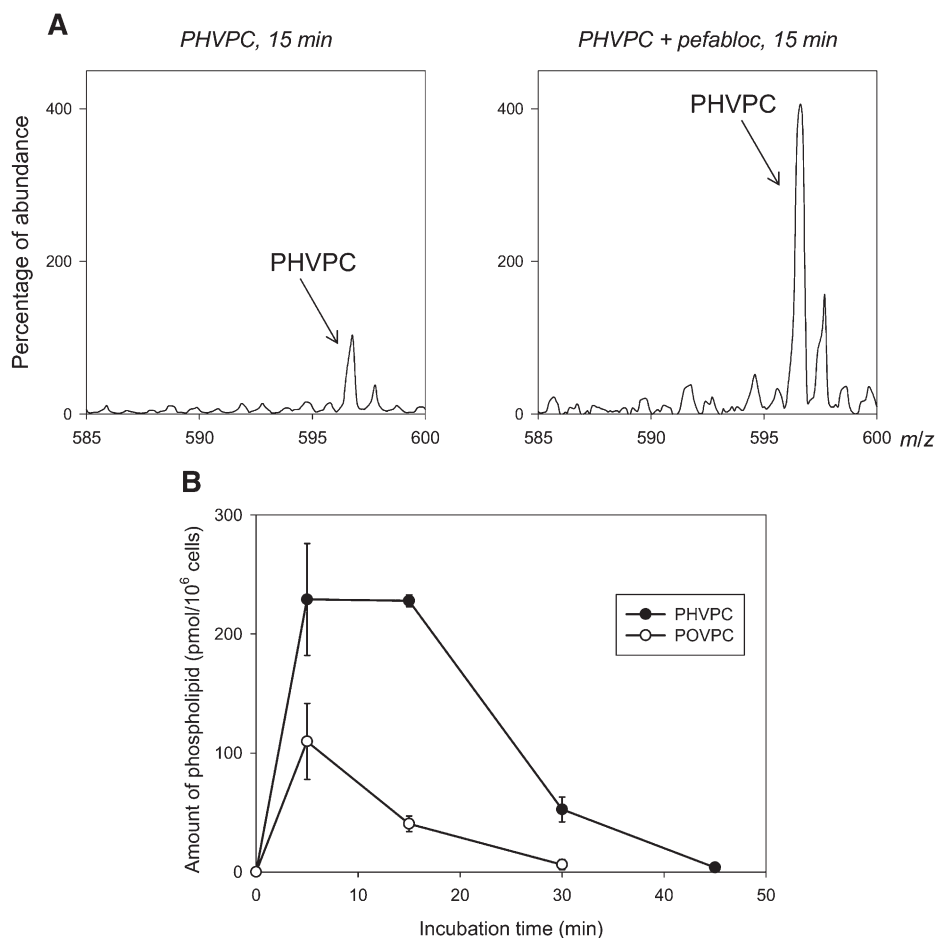
Fig. 5. Metabolism of PHVPC in THP-DM. (A) ESI mass spectra of the phospholipid fraction of THP-DM after 15 min incubation with 10 μM PHVPC in the absence or the presence of 50 μM pefabloc. Molecular ion due to unmetabolized PHVPC is indicated. (B) Retention of POVPC and PHVPC in THP-DM. Serum-starved cells were incubated with 10 μM POVPC or PHVPC in 2.5 ml HBSS. Incubation with the phospholipids was terminated at indicated intervals and the amount of POVPC or PHVPC remaining in the extract was determined using 1,2-dicaproyl-*sn*-glycerophosphocholine as standard. Data are mean ± SEM (n = 3).

The greater reactivity of PHVPC was also evident with MCP-1 and IL-6. Although both POVPC and lyso-PC were weak inducers, incubation with PHVPC led to a 15- to 150-fold greater increase in the expression of these genes (Fig. 6E, F). From these results, we conclude that PHVPC is significantly more effective than POVPC in inducing cytokine genes. Lyso-PC is more effective than POVPC, but it less potent than PHVPC.

The reactivity of POVPC and PHVPC may be related to their abbreviated *sn*-2 chains, which impart to these molecules a PAF-like character. However, the biological effects of PAF depend upon the *sn-3* phosphocholine head group. Hence, to determine whether the cytokine-inducing ability of POVPC and PHVPC is related to their choline head group, we prepared ethanolamine analogs of POVPC and PHVPC (i.e., POVPE and PHVPE). As shown in Fig. 6G, treatment with POVPE led to a 2- to 4-fold increase in the expression of IL-1β, IL-8, TNF-α, and MCP-1. The extent of increase in the expression of these genes was similar to that observed with POVPC. Moreover, like PHVPC, PH-VPE was markedly more potent than POVPE in increasing

cytokine gene expression, suggesting that the relative biological activities of these phospholipids are independent of the nature of the head group at the *sn*-3 position.

Metabolic regulation of the proinflammatory effects of POVPC: Our results so far indicated that the metabolites of POVPC are more active than the parent phospholipid. On the basis of these observations, we reasoned that inhibition of metabolism should decrease the proinflammatory effects of POVPC. To test this hypothesis, we examined the effects of inhibiting POVPC metabolism on cytokine gene induction. For these experiments, THP-1 cells were pretreated with either pefabloc or tolrestat for 1 h before the addition of POVPC, and changes in the expression of the IL-8 gene were measured 3 h after POVPC treatment. As before, treatment with POVPC led to a robust induction of IL-8 (**Fig. 7**). However, in the presence of pefabloc, the increase in IL-8 was 2-fold greater than in the absence of the inhibitor. This result suggests that inhibition of hydrolysis increases the biological activity of POVPC. Because lyso-PC was more reactive than POVPC (Fig. 6), this increase
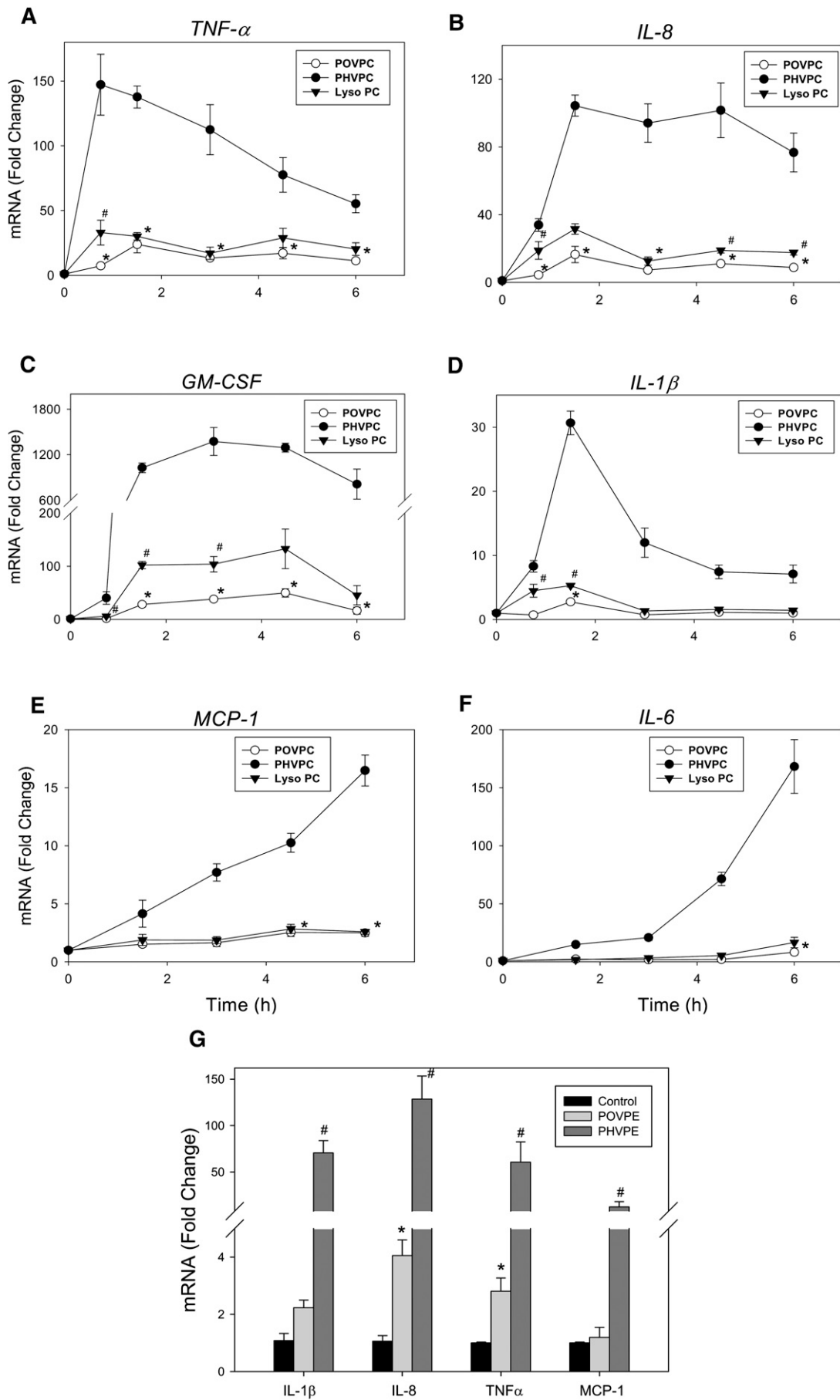
in cytokine gene induction could not be due to the accumulation of unmetabolized POVPC, but it might be due to increased accumulation of PHVPC (see Fig. 4).

In contrast to pefabloc, treatment with tolrestat led to a significant decrease in IL-8 induction. This observation suggests that inhibition of AR decreases PHVPC levels and therefore diminishes the overall reactivity of POVPC, even though lyso-PC formation is increased. To further confirm that the reactivity of POVPC depends upon PHVPC formation, the cells were treated directly by PHVPC. As before (see Fig. 6), PHVPC was more potent than POVPC in inducing IL-8; however, in pefabloc-treated cells, PHVPC was almost twice as effective as in untreated cells. The increase in the effect of PHVPC in the presence of pefabloc is consistent with the conclusion that PHVPC is more potent than lyso-PC. We suggest that by inhibiting hydrolysis, pefabloc prevents the removal of PHVPC (Fig. 5) and thereby increases cytokine production. Together, these results with inhibitors of AR and PLA$_2$ suggest that hydrolysis and reduction are competing pathways of POVPC metabolism (Scheme 1B-II) and that metabolism of POVPC increases its ability to induce cytokine genes.

Although studies with inhibitors (Figs. 4, 5, and 7), together with measurements of metabolites (Figs. 4 and 5), provide clear evidence that metabolism regulates inflammation, nonspecific effects of the inhibitors cannot be rigorously excluded. Hence, to examine the role of reduction, which appears to be the major bioactivating step in POVPC metabolism, we established macrophage cell lines from the bone marrow of wild-type (WT) and AR-null mice. These macrophage cell lines display the functional characteristics of primary cells and can be maintained in culture without an apparent change of phenotype for at least 10-12 passages. To examine their responses, WT and AR-null macrophages were treated with POVPC, and the induction of GM-CSF, TNF-α, and IL-1β genes was measured (**Fig. 8**). Treatment with POVPC for 3 h (but not 1.5 h) led to an 8.7-fold increase in GM-CSF mRNA, and a 20- to 23-fold increase in TNF-α and IL-1β mRNA. With TNF-α, 6.1-fold induction was observed within 1.5 h of incubation with POVPC. Compared with WT macrophages, no increase in the expression of GM-CSF was observed in AR-null macrophages. Although the expression of IL-1β and TNF-α was increased 2- to 3-fold even in AR-null macrophages compared with untreated cells, the overall extent of induction was significantly lower than the 20- to 25-fold increase observed with WT macrophages. These data are consistent with the results obtained with the AR inhibitor and support the view that metabolism via AR increases the proinflammatory effects of POVPC.

DISCUSSION

The major findings of this study are that the products of phospholipid oxidation, such as POVPC, increase the expression of cell survival and inflammatory genes in macrophages and that metabolism of these aldehydes increases their proinflammatory effects. We found that macrophages employ two major pathways to metabolize POVPC and related phospholipid aldehydes. Aldehyde phospholipids are either reduced by AR or they are hydrolyzed by PLA$_2$ to lyso-phospholipids. However, neither of these metabolic transformations decreases the proinflammatory effects of POVPC; instead, metabolites of both these pathways - PHVPC and lyso-PC - were found to be more effective in inducing cytokine gene expression than POVPC itself. Consistent with higher proinflammatory potential of PHVPC and lyso-PC, we found that blocking PLA$_2$-mediated hydrolysis leads to an accumulation of PHVPC and an increase in the induction of cytokine genes, whereas, inhibition of AR-mediated reduction led to a decrease in the proinflammatory effects of POVPC. Comparative studies showed that PHVPC was nearly an order-of-magnitude more active than either lyso-PC or POVPC; however, lyso-PC was more effective than POVPC. These observations provide new information about the mechanisms by which oxidized phospholipids induce inflammation and how their proinflammatory effects are regulated by metabolic transformation.

Previous studies suggest that phospholipid aldehydes generated during lipid oxidation play a key role in atherogenesis (4, 13). The process of atherogenesis begins with inflammation localized to lesion-prone areas containing subintimal depots of oxidized lipoproteins (2). It is believed vascular inflammation is triggered and maintained by bioactive component of oxidized LDL, particularly phospholipid aldehydes generated by oxygenation and bond-scission of sn-2 esterified unsaturated fatty acids. POVPC has been previously identified as one of the major oxidized phospholipids generated in oxidized LDL (5) and a key mediator of the atherogenic (6) and immunogenic (8–10, 23) effects of oxidized LDL.

Extensive research has uncovered a large number of cell signaling pathways that are activated by POVPC and related phospholipids (4, 13). Activation of these pathways leads to either proinflammatory or anti-inflammatory effects.

Fig. 6. Induction of cytokine genes by POVPC and its metabolites. Time-dependent changes in the expression of (A) TNF-α, (B) IL-8, (C) GM-CSF, (D) IL-1β, (E) MCP-1, and (F) IL-6 in THP-DM treated with 10 μM each of POVPC, lyso-PC, and PHVPC. (G) Changes in cytokine gene expression in THP-DM treated with 10 μM of POVPE or PHVPE for 3 h. The THP-1 cells were differentiated with 100 nM PMA for 72 h, incubated in media with 0.1% FBS for an additional 24 h, and then either left untreated or treated in HBSS with POVPC or POVPE and their metabolites. At indicated times, the cells were harvested, and their total RNA was extracted with RNeasy® Mini Kit (Qiagen). Changes in the levels of mRNA of cytokine genes were measured by quantitative RT-PCR as described in *Materials and Methods*. Data are mean ± SEM; n = 3. *$P < 0.05$ POVPC or POVPE versus untreated cell; [#]$P < 0.05$ Lyso-PC versus POVPC (A–F), or PHVPE versus POVPE-treated cells (G). PHVPC showed statistical significance ($P < 0.05$) versus untreated or POVPC-treated cells at all time points.
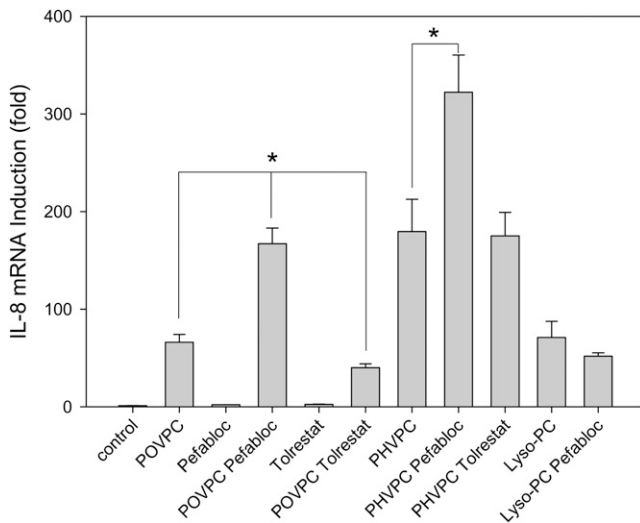
Fig. 7. Metabolic regulation of POVPC-induced changes in the expression of IL-8 gene. Relative changes in IL-8 induction in POVPC- or PHVPC-treated cells due to the inhibition of phospholipase A$_2$ or aldose reductase. Serum-starved THP-DM were either untreated or treated with 10 μM of POVPC, PHVPC, or lyso-PC without or with 50 μM of pefabloc or tolrestat, added 1 h before treatment with phospholipids. After 3 h of incubation with POVPC or PHVPC, the cells were harvested and changes in IL-8 mRNA were measured by qPT-PCR. Data are mean ± SEM; n = 3. *$P < 0.05$ versus POVPC or PHVPC as indicated.

In endothelial cells, the oxidized phospholipids increase cytokine production and promote monocyte binding. However, consistent with their electrophilic nature, oxidized phospholipids also activate Nrf2-dependent signaling (24, 25) resulting in the increase in phase II detoxification enzymes and protective proteins such as HO-1. They can also prevent the activation of NF-κB by TLR4 and thereby prevent lethal endotoxin shock in LPS-injected mice (26). The anti-inflammatory effects of oxidized phospholipids have been linked to their ability to bind directly to accessory proteins (CD15, MD2, and the LPS-binding protein) that interact with bacterial lipids (26, 27). However, the mechanisms responsible for the proinflammatory effects of oxidized lipids are less clear. Much of the work has been done in endothelial cells in which oxidized phospholipids increase monocyte binding by activating signaling cascades that involved activation of Rous sarcoma oncogene/Janus kinase/phosphatidylinositol 3 (src/JAK/PI3)- kinase, leading to the activation of endothelial nitric oxide synthase and sterol regulatory element binding protein (SREBP) (4). In macrophages, treatment with POVPC has been shown to increase cytokine production (28); however, the mechanism of this effect remains unclear.

In culture, human aortic endothelial cells respond to oxPAPC by upregulating more than 1,000 genes (29). Although prominent induction of IL-8 and genes involved in cholesterol metabolism and the unfolded protein response were observed, classical pathways of inflammation were not affected. In contrast, our studies with POVPC-exposed macrophages show a prominent increase in several proinflammatory cytokines, such as TNF-α, IL-6, IL-8, and IL-1β, that play a central role in inflammation. Thus, there may

be fundamental differences in the way in which different cells respond to oxidized phospholipids. Whereas endothelial cells seem to respond by increasing adhesion and cholesterol metabolism, the response in macrophages seems to be predominantly an increase in the expression of several cytokine genes. We found that exposure to POVPC upregulated the genes of several cytokines. There was also an increase in cytokines involved in chemoattraction of immature dendritic cells, memory T cells, and B cells [chemokine C-C motif ligand (CCL)20 (30) and MCP-1/CCL2 (31)] or those that increase monocyte mobilization and promote macrophage expansion (GM-CSF (32)). Significantly, exposure to POVPC led to a marked increase in genes involved in preventing apoptosis and promoting cell survival, such as baculoviral IAP repeat-containing (BIRC)3, BIRC2, BCL2-related protein (BCL2) A1, vascular endothelial growth factor (VEGF)-A, and insulin-like growth factor binding protein (IGFB)3. Both BIRC3 and BIRC2 are potent inhibitors of apoptosis that prevent proteolytic processing of procaspases by blocking cytochrome c-induced activation (33). BCL2A1 also reduces the release of cytochrome c and prevents caspase activation (34). Thus, the collective effects of the genomic changes induced by POVPC generated in the subintimal space are likely to result in monocyte recruitment and macrophage expansion within the lesion. Moreover, the induction of antiapoptotic genes by oxidized phospholipids may be one mechanism by which macrophages continue to survive in the toxic and hostile environment of advanced lesions.

Several of the genes induced by POVPC are direct targets of NF-κB (TNF-α, IL-6, IL-8, IL-1β, COX-2, and BCL2A1) or are induced by NF-κB-regulated genes such as TNF-α (CCL2, CCL20, BIRC2, and BIRC3). Indeed, in contrast to the effects of oxPAPC in endothelial cells, treatment of macrophages with POVPC led to an increase in NF-κB activation (data not shown), indicating that different cells respond differently to oxidized phospholipids. Nevertheless, several of the genes that were induced in macrophages are also expressed in high levels in atherosclerotic lesions. Abundant levels of TNF-α, IL-6, and IL-1β have been detected in the plaques of atherosclerotic animals (35). The expression of the GM-CSF receptor GMRα is elevated in atherosclerotic lesions, and GM-CSF has been found to play a key role in intimal cell proliferation in LDL-R-null mice (36). Similarly, MCP-1/CCL2 recruits monocytes to atheroma, and deletion of MCP-1 or its receptor CCR2 in atherosclerosis-susceptible mice prevents macrophage accumulation and decreases atherosclerotic lesion formation (37). Thus, exposure to POVPC elicits proinflammatory and proatherogenic responses in macrophages.

The findings of the current study demonstrate that the nature and the extent of inflammatory responses elicited by POVPC depend upon macrophage metabolism. POVPC and related phospholipids have an unusual *sn*-2 group, which due to its unique structure, alters membrane fluidity by disrupting the packing order of fatty acid chains in the phospholipid bilayer (38). The nature of this group is also important for the recognition of oxidized phospholipids
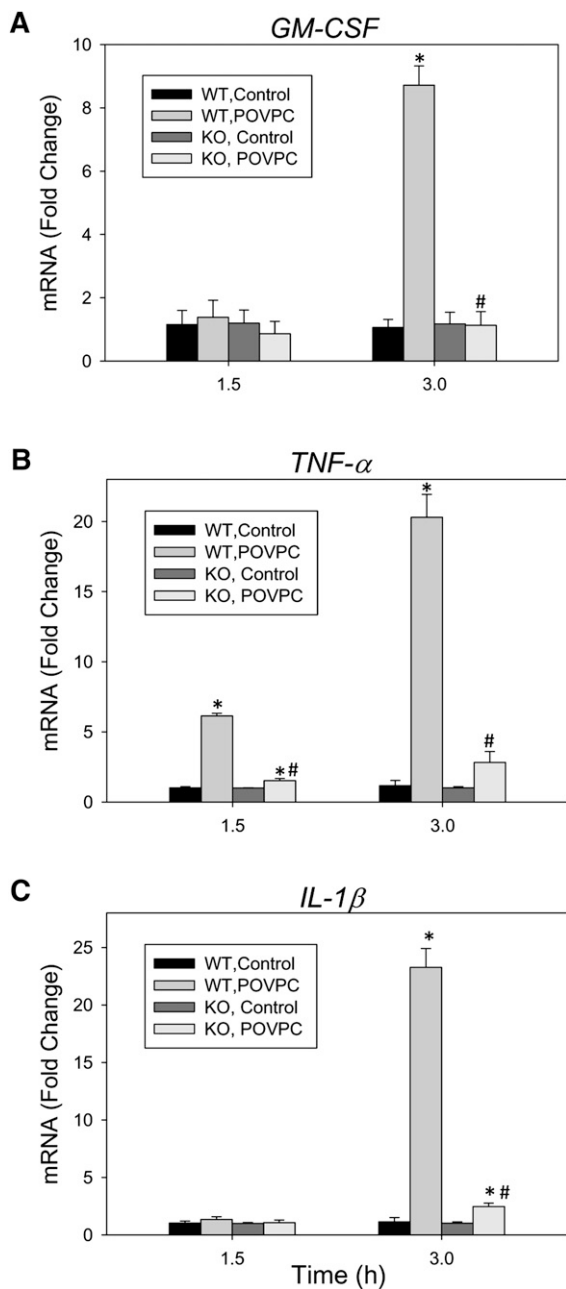
Fig. 8. Role of aldose reductase in regulating the induction of cytokine genes by POVPC. Relative changes in the expression of (A) GM-CSF, (B) TNF-α, and (C) IL-1β genes in WT and aldose reductase (AR)-null bone marrow derived macrophages. Cells were seeded in a 6-well plate, serum-starved for 24 h, and then treated with 10 μM POVPC for 1.5 or 3 h. After treatment, the cells were harvested and changes in mRNA were measured by real-time RT-PCR. Data are mean ± SEM; n = 3. *$P < 0.05$ versus untreated cells of the same genotype. #$P < 0.05$ WT versus KO.

by the PAF-receptor, scavenger receptor B-I, or CD36 (39, 40). Thus, changes in the structure of the sn-2 group during metabolism could drastically affect the biological activity of these phospholipids. Chemically, the sn-2 chain could be completely removed from the phospholipid by hydrolysis, or its ω-carbonyl could be enzymatically reduced or oxidized. In case of POVPC, we found that hydrolysis and reduction were the two major fates of the

phospholipid. No oxidative metabolism was detected in macrophages, although oxidation by aldehyde dehydrogenases remains an untested possibility in other cell types.

Hydrolysis of POVPC and related oxidized phospholipids with an abbreviated sn-2 chain has been shown to be catalyzed by PAF-acetylhydrolase (PAF-AH; group VIIA PLA₂). Two major forms of the enzyme have been described (41). The plasma form is secreted by cells of hematopoietic origin and is associated with circulating lipoproteins (Lp-PLA₂). The intracellular cytosolic form is expressed mainly in hepatocytes and epithelial cells of kidney and intestine (42). These phospholipases display high activity with sn-2 oxidized chains of phospholipids. In atherosclerotic lesions, Lp-PLA₂ is predominantly associated with macrophages localized to the lipid pool or the necrotic core of the lesion (43). Our results, which show for the first time that POVPC is extensively hydrolyzed in macrophages and that this hydrolysis is prevented by the serine esterase inhibitor pefabloc, indicate that macrophage PLA₂ plays a major role in the metabolism of oxidized phospholipids in macrophages.

In our study, hydrolysis of POVPC resulted in the formation of a lyso-PC, which was found to be more potent in stimulating cytokine production than POVPC, indicating that metabolism via PLA₂ may be important in increasing the proinflammatory effects of oxidized lipids. In clinical studies, Lp-PLA₂ is a robust predictor of cardiovascular disease risk independent of the established risk factors (41), and it has been suggested that under some clinical or experimental scenarios, Lp-PLA₂ may be a causal mediator of atherogenesis. Treatment of patients with angiographically documented coronary disease with the PLA₂ inhibitor darapladib has been reported to decrease the necrotic core volume of the plaque, a key determinant of plaque stability (44). Similarly, in a porcine model of diabetes and hypercholesterolemia, treatment with the PLA₂ inhibitor SB677116 was found to decrease inflammation and vascular accumulation of inflammatory cells (45). In contrast to its proatherogenic effects, PLA₂ has also been associated with a decrease in inflammation and a decrease in atherosclerotic lesion formation. For instance, gene transfer of Lp-PLA₂ in apoE-null mice led to a decrease in the deposition of oxidized lipoproteins and a reduction in atherosclerotic lesion formation in male (but not in female) mice (46). Similarly, local delivery of the Lp-PLA₂ gene at the site of injury decreases neointima formation in balloon-denuded aorta in cholesterol-fed rabbits (47) and inhibits the accumulation of oxidized lipoproteins and inflammation in normolipidemic rabbits (48). In addition, overexpression of PAF-AH in cells suppresses oxidative stress-induced cell death (49), whereas tissues from Pafah2-null mice display higher sensitivity to peroxide injury than tissues derived from WT mice (42).

Several reasons could account for the apparently contradictory effects of PLA₂ on inflammation and atherosclerosis. Difference may arise due to different study protocols; the location, association, or the extent of expression of the enzyme and the disease state; or the model and characteristics examined in the study. However, in all scenarios, the

product of PLA$_2$ hydrolysis of oxidized phospholipid will be a lyso-phospholipid, which in itself is not an innocuous metabolite. It induces apoptosis in endothelial cells (50), and it activates monocytes by increasing their production of inflammatory cytokines (IL-1β, IL-6, and TNF-α) (45). Our results support the inflammatory properties of lyso-PC, but more importantly, we demonstrate for the first time that lyso-PC is more active than the parent aldehyde phospholipid POVPC. This finding suggests that the metabolism via PLA$_2$ could increase inflammation, at least in macrophages exposed to oxidized phospholipids. Although the activities of other oxidized phospholipids relative to their lyso-phospholipids were not examined, the observation that inhibition of PLA$_2$ abrogates the inflammatory responses to oxidized LDL in monocytes suggests that the overall effect of the hydrolysis of oxidized phospholipids by PLA$_2$ is to increase rather than decrease inflammation.

Even though its products (lyso-phospholipids) have greater inflammatory activity than parent phospholipids, PLA$_2$ could potentially prevent both inflammation and atherosclerosis. We found that inhibition of PLA$_2$ increased the accumulation of PHVPC. Because PHVPC was more active than either lyso-PC or POVPC, it is likely that under some conditions, inhibition of PLA$_2$ could exacerbate inflammation if there is a subsidiary pathway of metabolism that enhances the biological activity of the oxidized phospholipid. Thus, a significant conclusion from our work is that PLA$_2$ is not the only biochemical pathway for the metabolism of oxidized lipids and that there may be subsidiary, interdependent pathways of metabolism that could significantly and robustly modify the effects of oxidized lipids and the role of PLA$_2$ in regulating both inflammation and atherosclerosis.

In case of macrophages, this subsidiary pathway was catalyzed by AR. This enzyme has broad substrate specificity and near-ubiquitous expression (51). Our previous studies have shown that AR and related members of the AKR superfamily are efficient catalysts for the reduction of POVPC and other phospholipid aldehydes (15, 17). Our current study confirms this activity and extends it to the metabolism of POVPC in macrophages. In addition, we found that the AR-catalyzed pathway competes with PLA$_2$ hydrolysis for the POVPC metabolism, but the product of this pathway, PHVPC, is also hydrolyzed by PLA$_2$. Thus, even though the eventual fate of POVPC is hydrolysis, the side reaction with AR serves to increase the inflammatory capacity of the phospholipid. Therefore, reduction by AR could be viewed as a sensory pathway by which the inflammatory effect of oxidized phospholipids could be amplified. The inflammation-enhancing role of this pathway is consistent with previous studies showing that inhibition of AR prevents NF-κB activation (52) and cellular or systemic inflammation induced by high glucose (53), TNF-α (54), or LPS (55). In agreement with these findings, we observed that inhibition of AR led to a significant suppression of POVPC-induced cytokine production. Nevertheless, how the products of AR, such as PHVPC, trigger changes in cytokine gene expression remains unknown.

Because PHVPC retains the PAF-like structure of the molecule, it could be speculated that PHVPC is also recognized by the same receptors as is POVPC (CD36, SRB-I, PAF-R), and because the loss of the reactive ω-carbonyl makes PHVPC less likely to react nonenzymatically with cellular nucleophiles, PHVPC may be a more stable ligand of these receptors than POVPC. Indeed, our studies show that the lifetime of PHVPC in macrophages was significantly longer than the lifetime of POVPC (Fig. 5C), indicating that PHVPC may cause a stronger and/or more sustained activation of cellular receptors than POVPC.

The efficacy of the reductive metabolism of POVPC in mediating inflammatory changes is likely to depend upon the relative level of expression and activity of both AR and PLA$_2$ rather than the absolute activity of each of this enzyme. Thus, even in cells replete with AR, the extent of inflammation induced will be minimal if these cells also express high levels of PLA$_2$, and vice versa. In addition, the levels of the specific receptors that recognize lyso-PC and PHVPC will be important. In cells that lack receptors for PHVPC or lyso-PC (but not those that recognize POVPC), metabolism via PLA$_2$ or AR may actually lead to decrease in inflammation. For instance, in contrast to the proinflammatory effect of lyso-PC and PHVPC described here, Subbanagounder et al. reported that hydrolysis by PLA$_2$ or reduction by sodium borohydride led to a significant decrease in the ability of POVPC to enhance leukocyte-endothelial interactions (6). Thus, it is possible that different cells sense the presence of oxidized phospholipids by different mechanisms and that the difference in metabolic pathways or cellular receptors allows them to respond differently to oxidized phospholipids. As a result, the in vivo effects of the oxidized phospholipids on inflammation are difficult to predict from direct extrapolation of in vitro data.

There is even greater difficulty in evaluating the in vivo atherogenic significance of this metabolism and its inflammatory consequences. The relationship between inflammation and atherogenesis is complex, and although high levels of inflammation in advanced lesions is associated in an increase in plaque vulnerability, inhibition of inflammation does not always decrease lesion formation. For example, in LDL-R null mice, inhibition of NF-κB in macrophages decreases atherosclerotic lesion formation (56), whereas IL-6-null mice develop more fatty streaks than WT mice (57). Similarly, despite the clear inflammation-enhancing effects of PLA$_2$ and AR in macrophages reported here, atherosclerotic lesion formation is higher in AR- and apoE-null mice than it is in WT-apoE-null mice (58), and Lp-PLA$_2$ gene transfer reduces spontaneous atherosclerosis (46). Clearly, extensive additional investigations are required to fully understand how inflammation contributes to atherosclerotic lesion formation and how it is triggered by oxidized phospholipids and regulated by their metabolism.

In summary, the results of this study show that in macrophages, phospholipid aldehydes such as POVPC are metabolized by two distinct but interrelated metabolic pathways catalyzed by PLA$_2$ and AR. Products of both these pathways (lyso-PC and PHVPC) were more effective in inducing the expression of cytokine genes than was unmetabolized

POVPC. Inhibition of PLA$_2$ led to the accumulation of POVPC and PHVPC and increased cytokine gene expression. The induction of cytokine genes was diminished by inhibiting AR in macrophages from AR-null mice. These findings provide a new understanding of the proinflammatory effects of oxidized phospholipids and how they are regulated by cellular metabolism. ⬛

REFERENCES

1. Lloyd-Jones, D., R. J. Adams, T. M. Brown, M. Carnethon, S. Dai, G. De Simone, T. B. Ferguson, E. Ford, K. Furie, C. Gillespie, et al. 2010. Heart disease and stroke statistics–2010 update: a report from the American Heart Association. *Circulation.* **121:** e46–e215.
2. Glass, C. K., and J. L. Witztum. 2001. Atherosclerosis. the road ahead. *Cell.* **104:** 503–516.
3. Hansson, G. K., and P. Libby. 2006. The immune response in atherosclerosis: a double-edged sword. *Nat. Rev. Immunol.* **6:** 508–519.
4. Berliner, J. A., N. Leitinger, and S. Tsimikas. 2009. The role of oxidized phospholipids in atherosclerosis. *J. Lipid Res.* **50(Suppl):** S207–S212.
5. Watson, A. D., N. Leitinger, M. Navab, K. F. Faull, S. Horkko, J. L. Witztum, W. Palinski, D. Schwenke, R. G. Salomon, W. Sha, et al. 1997. Structural identification by mass spectrometry of oxidized phospholipids in minimally oxidized low density lipoprotein that induce monocyte/endothelial interactions and evidence for their presence in vivo. *J. Biol. Chem.* **272:** 13597–13607.
6. Subbanagounder, G., N. Leitinger, D. C. Schwenke, J. W. Wong, H. Lee, C. Rizza, A. D. Watson, K. F. Faull, A. M. Fogelman, and J. A. Berliner. 2000. Determinants of bioactivity of oxidized phospholipids. Specific oxidized fatty acyl groups at the sn-2 position. *Arterioscler. Thromb. Vasc. Biol.* **20:** 2248–2254.
7. Itabe, H., E. Takeshima, H. Iwasaki, J. Kimura, Y. Yoshida, T. Imanaka, and T. Takano. 1994. A monoclonal antibody against oxidized lipoprotein recognizes foam cells in atherosclerotic lesions. Complex formation of oxidized phosphatidylcholines and polypeptides. *J. Biol. Chem.* **269:** 15274–15279.
8. Palinski, W., S. Horkko, E. Miller, U. P. Steinbrecher, H. C. Powell, L. K. Curtiss, and J. L. Witztum. 1996. Cloning of monoclonal autoantibodies to epitopes of oxidized lipoproteins from apolipoprotein E-deficient mice. Demonstration of epitopes of oxidized low density lipoprotein in human plasma. *J. Clin. Invest.* **98:** 800–814.
9. Tsimikas, S., E. S. Brilakis, E. R. Miller, J. P. McConnell, R. J. Lennon, K. S. Kornman, J. L. Witztum, and P. B. Berger. 2005. Oxidized phospholipids, Lp(a) lipoprotein, and coronary artery disease. *N. Engl. J. Med.* **353:** 46–57.
10. Tsimikas, S., S. Kiechl, J. Willeit, M. Mayr, E. R. Miller, F. Kronenberg, Q. Xu, C. Bergmark, S. Weger, F. Oberhollenzer, et al. 2006. Oxidized phospholipids predict the presence and progression of carotid and femoral atherosclerosis and symptomatic cardiovascular disease: five-year prospective results from the Bruneck study. *J. Am. Coll. Cardiol.* **47:** 2219–2228.
11. Lee, H., W. Shi, P. Tontonoz, S. Wang, G. Subbanagounder, C. C. Hedrick, S. Hama, C. Borromeo, R. M. Evans, J. A. Berliner, et al. 2000. Role for peroxisome proliferator-activated receptor alpha in oxidized phospholipid-induced synthesis of monocyte chemotactic protein-1 and interleukin-8 by endothelial cells. *Circ. Res.* **87:** 516–521.
12. Leitinger, N., T. R. Tyner, L. Oslund, C. Rizza, G. Subbanagounder, H. Lee, P. T. Shih, N. Mackman, G. Tigyi, M. C. Territo, et al. 1999. Structurally similar oxidized phospholipids differentially regulate endothelial binding of monocytes and neutrophils. *Proc. Natl. Acad. Sci. USA.* **96:** 12010–12015.
13. Berliner, J. A., and N. M. Gharavi. 2008. Endothelial cell regulation by phospholipid oxidation products. *Free Radic. Biol. Med.* **45:** 119–123.
14. Furnkranz, A., A. Schober, V. N. Bochkov, P. Bashtrykov, G. Kronke, A. Kadl, B. R. Binder, C. Weber, and N. Leitinger. 2005. Oxidized phospholipids trigger atherogenic inflammation in murine arteries. *Arterioscler. Thromb. Vasc. Biol.* **25:** 633–638.
15. Spite, M., S. P. Baba, Y. Ahmed, O. A. Barski, K. Nijhawan, J. M. Petrash, A. Bhatnagar, and S. Srivastava. 2007. Substrate specificity and catalytic efficiency of aldo-keto reductases with phospholipid aldehydes. *Biochem. J.* **405:** 95–105.
16. Tabas, I. 2010. Macrophage death and defective inflammation resolution in atherosclerosis. *Nat. Rev. Immunol.* **10:** 36–46.
17. Srivastava, S., M. Spite, J. O. Trent, M. B. West, Y. Ahmed, and A. Bhatnagar. 2004. Aldose reductase-catalyzed reduction of aldehyde phospholipids. *J. Biol. Chem.* **279:** 53395–53406.
18. Chen, P. S., T. Y. Toribara, and H. Warner. 1956. Microdetermination of phosporus. *Anal. Chem.* **28:** 1756–1758.
19. Clemons-Miller, A. R., G. W. Cox, J. Suttles, and R. D. Stout. 2000. LPS stimulation of TNF-receptor deficient macrophages: a differential role for TNF-alpha autocrine signaling in the induction of cytokine and nitric oxide production. *Immunobiology.* **202:** 477–492.
20. Bligh, E. G., and W. J. Dyer. 1959. A rapid method of total lipid extraction and purification. *Can. J. Biochem. Physiol.* **37:** 911–917.
21. Boullier, A., K. L. Gillotte, S. Horkko, S. R. Green, P. Friedman, E. A. Dennis, J. L. Witztum, D. Steinberg, and O. Quehenberger. 2000. The binding of oxidized low density lipoprotein to mouse CD36 is mediated in part by oxidized phospholipids that are associated with both the lipid and protein moieties of the lipoprotein. *J. Biol. Chem.* **275:** 9163–9169.
22. Hayashi, A., T. Matsubara, M. Morita, T. Kinoshita, and T. Nakamura. 1989. Structural analysis of choline phospholipids by fast atom bombardment mass spectrometry and tandem mass spectrometry. *J. Biochem.* **106:** 264–269.
23. Tsimikas, S., M. Aikawa, F. J. Miller, Jr., E. R. Miller, M. Torzewski, S. R. Lentz, C. Bergmark, D. D. Heistad, P. Libby, and J. L. Witztum. 2007. Increased plasma oxidized phospholipid:apolipoprotein B-100 ratio with concomitant depletion of oxidized phospholipids from atherosclerotic lesions after dietary lipid-lowering: a potential biomarker of early atherosclerosis regression. *Arterioscler. Thromb. Vasc. Biol.* **27:** 175–181.
24. Jyrkkänen, H. K., E. Kansanen, M. Inkala, A. M. Kivela, H. Hurttila, S. E. Heinonen, G. Goldsteins, S. Jauhiainen, S. Tiainen, H. Makkonen, et al. 2008. Nrf2 regulates antioxidant gene expression evoked by oxidized phospholipids in endothelial cells and murine arteries in vivo. *Circ. Res.* **103:** e1–e9.
25. Kadl, A., A. K. Meher, P. R. Sharma, M. Y. Lee, A. C. Doran, S. R. Johnstone, M. R. Elliott, F. Gruber, J. Han, W. Chen, et al. 2010. Identification of a novel macrophage phenotype that develops in response to atherogenic phospholipids via Nrf2. *Circ. Res.* **107:** 737–746.
26. Bochkov, V. N., A. Kadl, J. Huber, F. Gruber, B. R. Binder, and N. Leitinger. 2002. Protective role of phospholipid oxidation products in endotoxin-induced tissue damage. *Nature.* **419:** 77–81.
27. Erridge, C., S. Kennedy, C. M. Spickett, and D. J. Webb. 2008. Oxidized phospholipid inhibition of toll-like receptor (TLR) signaling is restricted to TLR2 and TLR4: roles for CD14, LPS-binding protein, and MD2 as targets for specificity of inhibition. *J. Biol. Chem.* **283:** 24748–24759.
28. Pégorier, S., D. Stengel, H. Durand, M. Croset, and E. Ninio. 2006. Oxidized phospholipid: POVPC binds to platelet-activating-factor receptor on human macrophages. Implications in atherosclerosis. *Atherosclerosis.* **188:** 433–443.
29. Gargalovic, P. S., M. Imura, B. Zhang, N. M. Gharavi, M. J. Clark, J. Pagnon, W. P. Yang, A. He, A. Truong, S. Patel, et al. 2006. Identification of inflammatory gene modules based on variations of human endothelial cell responses to oxidized lipids. *Proc. Natl. Acad. Sci. USA.* **103:** 12741–12746.
30. Schutyser, E., S. Struyf, and J. Van Damme. 2003. The CC chemokine CCL20 and its receptor CCR6. *Cytokine Growth Factor Rev.* **14:** 409–426.
31. Rot, A., and U. H. von Andrian. 2004. Chemokines in innate and adaptive host defense: basic chemokinese grammar for immune cells. *Annu. Rev. Immunol.* **22:** 891–928.
32. Hamilton, J. A. 2008. Colony-stimulating factors in inflammation and autoimmunity. *Nat. Rev. Immunol.* **8:** 533–544.
33. Deveraux, Q. L., N. Roy, H. R. Stennicke, T. Van Arsdale, Q. Zhou, S. M. Srinivasula, E. S. Alnemri, G. S. Salvesen, and J. C. Reed. 1998.

IAPs block apoptotic events induced by caspase-8 and cytochrome c by direct inhibition of distinct caspases. *EMBO J.* **17:** 2215–2223.

34. Vogler, M., D. Dinsdale, M. J. Dyer, and G. M. Cohen. 2009. Bcl-2 inhibitors: small molecules with a big impact on cancer therapy. *Cell Death Differ.* **16:** 360–367.

35. Kleemann, R., S. Zadelaar, and T. Kooistra. 2008. Cytokines and atherosclerosis: a comprehensive review of studies in mice. *Cardiovasc. Res.* **79:** 360–376.

36. Zhu, S. N., M. Chen, J. Jongstra-Bilen, and M. I. Cybulsky. 2009. GM-CSF regulates intimal cell proliferation in nascent atherosclerotic lesions. *J. Exp. Med.* **206:** 2141–2149.

37. Charo, I. F., and M. B. Taubman. 2004. Chemokines in the pathogenesis of vascular disease. *Circ. Res.* **95:** 858–866.

38. Rhode, S., R. Grurl, M. Brameshuber, A. Hermetter, and G. J. Schutz. 2009. Plasma membrane fluidity affects transient immobilization of oxidized phospholipids in endocytotic sites for subsequent uptake. *J. Biol. Chem.* **284:** 2258–2265.

39. Kar, N. S., M. Z. Ashraf, M. Valiyaveettil, and E. A. Podrez. 2008. Mapping and characterization of the binding site for specific oxidized phospholipids and oxidized low density lipoprotein of scavenger receptor CD36. *J. Biol. Chem.* **283:** 8765–8771.

40. Gao, D., M. Z. Ashraf, N. S. Kar, D. Lin, L. M. Sayre, and E. A. Podrez. 2010. Structural basis for the recognition of oxidized phospholipids in oxidized low density lipoproteins by class B scavenger receptors CD36 and SR-BI. *J. Biol. Chem.* **285:** 4447–4454.

41. Tellis, C. C., and A. D. Tselepis. 2009. The role of lipoprotein-associated phospholipase A2 in atherosclerosis may depend on its lipoprotein carrier in plasma. *Biochim. Biophys. Acta.* **1791:** 327–338.

42. Kono, N., T. Inoue, Y. Yoshida, H. Sato, T. Matsuse, H. Itabe, E. Niki, J. Aoki, and H. Arai. 2008. Protection against oxidative stress-induced hepatic injury by intracellular type II platelet-activating factor acetylhydrolase by metabolism of oxidized phospholipids in vivo. *J. Biol. Chem.* **283:** 1628–1636.

43. Kolodgie, F. D., A. P. Burke, K. S. Skorija, E. Ladich, R. Kutys, A. T. Makuria, and R. Virmani. 2006. Lipoprotein-associated phospholipase A2 protein expression in the natural progression of human coronary atherosclerosis. *Arterioscler. Thromb. Vasc. Biol.* **26:** 2523–2529.

44. Serruys, P. W., H. M. Garcia-Garcia, P. Buszman, P. Erne, S. Verheye, M. Aschermann, H. Duckers, O. Bleie, D. Dudek, H. E. Botker, et al. 2008. Effects of the direct lipoprotein-associated phospholipase A(2) inhibitor darapladib on human coronary atherosclerotic plaque. *Circulation.* **118:** 1172–1182.

45. Shi, Y., P. Zhang, L. Zhang, H. Osman, E. R. Mohler 3rd, C. Macphee, A. Zalewski, A. Postle, and R. L. Wilensky. 2007. Role of lipoprotein-associated phospholipase A2 in leukocyte activation and inflammatory responses. *Atherosclerosis.* **191:** 54–62.

46. Quarck, R., B. De Geest, D. Stengel, A. Mertens, M. Lox, G. Theilmeier, C. Michiels, M. Raes, H. Bult, D. Collen, et al. 2001. Adenovirus-mediated gene transfer of human platelet-activating factor-acetylhydrolase prevents injury-induced neointima formation and reduces spontaneous atherosclerosis in apolipoprotein E-deficient mice. *Circulation.* **103:** 2495–2500.

47. Turunen, P., H. Puhakka, J. Rutanen, M. O. Hiltunen, T. Heikura, M. Gruchala, and S. Yla-Herttuala. 2005. Intravascular adenovirus-mediated lipoprotein-associated phospholipase A2 gene transfer reduces neointima formation in balloon-denuded rabbit aorta. *Atherosclerosis.* **179:** 27–33.

48. Arakawa, H., J. Y. Qian, D. Baatar, K. Karasawa, Y. Asada, Y. Sasaguri, E. R. Miller, J. L. Witztum, and H. Ueno. 2005. Local expression of platelet-activating factor-acetylhydrolase reduces accumulation of oxidized lipoproteins and inhibits inflammation, shear stress-induced thrombosis, and neointima formation in balloon-injured carotid arteries in nonhyperlipidemic rabbits. *Circulation.* **111:** 3302–3309.

49. Matsuzawa, A., K. Hattori, J. Aoki, H. Arai, and K. Inoue. 1997. Protection against oxidative stress-induced cell death by intracellular platelet-activating factor-acetylhydrolase II. *J. Biol. Chem.* **272:** 32315–32320.

50. Takahashi, M., H. Okazaki, Y. Ogata, K. Takeuchi, U. Ikeda, and K. Shimada. 2002. Lysophosphatidylcholine induces apoptosis in human endothelial cells through a p38-mitogen-activated protein kinase-dependent mechanism. *Atherosclerosis.* **161:** 387–394.

51. Srivastava, S. K., K. V. Ramana, and A. Bhatnagar. 2005. Role of aldose reductase and oxidative damage in diabetes and the consequent potential for therapeutic options. *Endocr. Rev.* **26:** 380–392.

52. Ramana, K. V., D. Chandra, S. Srivastava, A. Bhatnagar, B. B. Aggarwal, and S. K. Srivastava. 2002. Aldose reductase mediates mitogenic signaling in vascular smooth muscle cells. *J. Biol. Chem.* **277:** 32063–32070.

53. Ramana, K. V., A. Bhatnagar, and S. K. Srivastava. 2004. Inhibition of aldose reductase attenuates TNF-alpha-induced expression of adhesion molecules in endothelial cells. *FASEB J.* **18:** 1209–1218.

54. Ramana, K. V., R. Tammali, A. B. Reddy, A. Bhatnagar, and S. K. Srivastava. 2007. Aldose reductase-regulated tumor necrosis factor-alpha production is essential for high glucose-induced vascular smooth muscle cell growth. *Endocrinology.* **148:** 4371–4384.

55. Ramana, K. V., M. S. Willis, M. D. White, J. W. Horton, J. M. DiMaio, D. Srivastava, A. Bhatnagar, and S. K. Srivastava. 2006. Endotoxin-induced cardiomyopathy and systemic inflammation in mice is prevented by aldose reductase inhibition. *Circulation.* **114:** 1838–1846.

56. Kanters, E., M. Pasparakis, M. J. Gijbels, M. N. Vergouwe, I. Partouns-Hendriks, R. J. Fijneman, B. E. Clausen, I. Forster, M. M. Kockx, K. Rajewsky, et al. 2003. Inhibition of NF-kappaB activation in macrophages increases atherosclerosis in LDL receptor-deficient mice. *J. Clin. Invest.* **112:** 1176–1185.

57. Van Lenten, B. J., A. C. Wagner, M. Navab, and A. M. Fogelman. 2001. Oxidized phospholipids induce changes in hepatic paraoxonase and ApoJ but not monocyte chemoattractant protein-1 via interleukin-6. *J. Biol. Chem.* **276:** 1923–1929.

58. Srivastava, S., E. Vladykovskaya, O. A. Barski, M. Spite, K. Kaiserova, J. M. Petrash, S. S. Chung, G. Hunt, B. Dawn, and A. Bhatnagar. 2009. Aldose reductase protects against early atherosclerotic lesion formation in apolipoprotein E-null mice. *Circ. Res.* **105:** 793–802.